Institut for Bærende Konstruktioner og Materialer
Department of Structural Engineering and Materials
Danmarks Tekniske Universitet • Technical University of Denmark

BKM

Fatigue in Welded Connections

A new approach to predict crack propagation behaviour

Thomas Cornelius Hansen

Serie R No 10 1996

Fatigue in Welded Connections. A new approach to predict crack propagation behaviour.

Tryk:
LTT
Danmarks Tekniske Universitet
Lyngby
ISBN 87-7740-190-5
ISSN 1396-2167
Bogbinder:
H. Meyer, Bygning 101, DTU

I Contents

II Preface

This report has been prepared as one part of the thesis required to obtain the Ph.d. degree at the Technical University of Denmark. The report is the result of a research project carried out at the Department of Structural Engineering, under the supervision of Prof.dr.techn M.P.Nielsen.

The project has been financed by Statens Teknisk Videnskabelige Forskningsråd.

This report deals with fracture mechanics in welded connections. The main subjects are crack propagation under fatigue loading and presentation and evaluation of a newly developed theory, which is able to predict crack propagation under dynamic loading.

I would like to thank my supervisor for giving valuable inspiration and encouragement during the project.

Finally I express my gratitude to all other persons, who contributed to the completion of this report.

Lyngby, november 1996

Thomas Cornelius Hansen

III Abstract

The main purpose of this paper is to test a new theory of crack propagation by comparing it's results with test results from welded connections. The advantage of the new theory is that crack propagation may be predicted on the basis of knowledge of well-known material parameters, contrary to the empirical formulas, the parameters of which must be determined by time consuming fatigue tests.

The paper is divided into four main parts:
-Presentation of the new theory (chapter 2)
-Basic concepts concerning welded connections (chapter 3)
-Presentation of test results (chapter 4)
-Predicting crack propagation using the new theory, and comparing the theory with test results (chapter 5)

The theory is compared with two types of tests, using the da/dN-ΔK_I and the S-N concept respectively.
Firstly a tests series performed by Glinka **[79.1]** is chosen because it very clearly shows how the crack velocity da/dN depends on the type of weld in the plates. The test specimen is a standard Welded Center Cracked Test specimens (WCCT) welded together in different directions compared to the crack propagation direction. This results in different residual stress fields in the specimens and the capability of the Crack Propagation Formula to predict the effect from this is examined. Secondly a test series with welded joints (WJT) performed by Ibsø **[92.1]** is investigated. The test series has been chosen because the welded joint plates are very similar to those used in real structures, as for example off shore structures. It is examined whether the Crack Propagation Formula is able to predict the crack propagation and determine the fatigue life of the specimens.
The report touches upon subjects like residual stresses, the so-called R ratio and crack closure when evaluating the new theory.

IV Resume

Hovedformålet med denne afhandling er at eftervise en nyudviklet revnevækst-teori ved at sammenholde dens resultater med forsøg i svejste samlinger. Fordelen ved den nye teori er, at den er baseret på velkendte materialeparametre, ikke på empiriske konstanter udledt ved tidskrævende udmattelsesforsøg.

Afhandlingen er inddelt i fire hoveddele:
-Præsentation af den nye teori (kap.2)
-Grundlæggende koncepter for svejste samlinger (kap.3)
-Præsentation af forsøgsresultater (kap.4)
-Beregning af revnevækst vha den ny teori og
sammenligning af teori med forsøg (kap.5)

Teorien er sammenlignet med to forsøgsserier, ved at benytte henholdsvis da/dN-ΔK_I og S-N kurve koncepterne.
Først behandles en forsøgsserie udført af Glinka **[79.1]**. Den er valgt fordi den meget tydeligt viser, hvordan revnevækstændringen da/dN afhænger af typen af svejste samlinger i plader. Forsøgsprøveemnerne er af typen Welded Center Cracked Test specimens (WCCT) svejst sammen i forskellige retninger i forhold til revnevækstretningen. Dette resulterer i forskellige egenspændingsfelter i prøveemnerne og det vil blive undersøgt om revnevækstformlen er i stand til at forudsige denne effekt.
Dernæst undersøges en forsøgsserie med svejste samlinger (WJT) udført af Ibsø **[92.1]**. Denne forsøgsserie er valgt fordi forsøgsemnerne ligner svejste samlinger i virkelige konstruktioner, som for eksempel off-shore konstruktioner. Det er undersøgt om revnevækstformlen er i stand til at forudsige revnevæksten og fastlægge prøvemnernes udmattelseslevetid.
Generelt vil emner som egenspændinger, R forholdet og revnelukning blive behandlet i afhandlingen.

V Notations

a	Crack length
a_i	Initial crack length
a_f	Crack length at failure
a'_p	Fracture zone length
a_y	Plastic zone length
l_e	Crack length correction
a_{eff}	Effective crack length
B,t	Thickness
W	Width, Elastic energy
L	Length
H	Height
D	Diameter
r	Radius, Length
A	Area
V	Volume
N	Number of cyclic load steps

N_i	Number of cycles to initation
N_p	Number of cycles in the crack propagation phase
N_f	Number of cycles to failure
da/dN	Crack growth rate
P	Force
P_{min}	Minimum Force
P_{max}	Maximum Force
ΔP	Force increment under dynamic load (P_{max}-P_{min})
R	Stress ratio $\sigma_{min}/\sigma_{max}$
σ	Normal stress
σ_{min}	Minimum stress
σ_{max}	Maximum stress
$\Delta\sigma$	Stress increment under dynamic load (σ_{max}-σ_{min})
σ_r^{yy}	Residual stress
S	Stress
S_o	Crack opening stress
f_u	Ultimate stress
f_y	Yield stress

f_t	Tensile strength or true fracture strength
u	Displacement
ϵ	Longitudinal strain
E	Modulus of Elasticity (Youngs modulus)
K_I	Stress intensity factor
K_{Imin}	Stress intensity factor at minimum stress
K_{Imax}	Stress intensity factor at maximum stress
K_r	Stress intensity factor in a residual stress field
K_s	Stress intensity factor from external load
ΔK_I	Stress intensity factor increment under dynamic load (K_{Imax}-K_{Imin})
K_{op}	Crack opening stress intensity factor
ΔK_{eff}	Effective stress intensity factor
K_{th}	Threshold value of stress intensity factor
K_{IC}	Critical stress intensity factor
SCF	Elastic stress intensity factor at the weld toe
h(x)	Weight function
G_F	Fracture energy
U	Energy release rate

C,m	Empirical constants in Paris equation
d,q	Empirical constants, related to the geometrical correction factor F_G
c,n	Empirical constants, Weibull size effect parameters
M',n'	Empirical constants, K_{IC} - K_I relation
η	R-ratio correction factor
β	Stress intensity correction factor
F_S,F_E,F_T,F_G	Stress intensity correction factors

Chapter 1

Introduction

Over several decades it has been known that many metal components and structures fail in service, even though they are capable of withstanding considerably higher loads if the loads are of a static nature. The failure type involved is governed by crack propagation caused by fatigue loading.
Crack formation needs a void or notch in the structure for starting propagate. In welded connections this void, also called the initial crack, is often due to the heating of the base material before welding. Welded connections in structures are almost inevitable. Therefore it is obvious that most structures fail from fatigue. In fact the service life of metal structures in about 90% of the cases is terminated due to fatigue failure.
Normally fatigue failure is studied by using empirical formulas, as for instance the well-known Paris equation **[63.1]**. To use this formula it is necessary to determine crack growth parameters by time demanding and expensive tests. Since fatigue failure indeed is a serious problem, it is of vital interest for the society to have a simple tool to determine the service life of structures. At the Department of Structural Engineering, an energy balance crack propagation formula has been developed **[90.1]**. This formula can be used to predict crack propagation arising both from static load and from fatigue loading. The potential power of a theoretical formula is that it is not necessary to determine crack growth parameters by time demanding and expensive tests, as is the case when empirical formulas are used. The formula will be described shortly in the next chapter.
The main purpose of this paper is to examine the capability of the new formula to predict crack propagation in welded connections. A comparison with two kinds of welded connections will be carried out. Firstly a comparison with a test series of the type Welded Center Cracked Test specimens (WCCT) will be performed using the da/dN-ΔK_I curve approach to compare the test results with the theory. Secondly a comparison with tests with Fillet Welded Joint Test specimens (WJT) will be performed using the S-N-diagram approach when comparing with theory.

Chapter 2

The energy balance crack propagation formula

2.1 Introduction

This chapter contains a short introduction to the energy balance crack propagation formula. A more detailed description may be found in **[90.1]**. The formula is based upon an energy criterion and modified linear elastic fracture mechanics (LEFM). This leads to a differential equation of first order, which is difficult to solve analytically. Instead it may be solved by use of numerical methods.

2.2 Irwins crack length correction

As well known from linear elastic fracture mechanics, the normal stress σ_y along the axis of a sharp crack is governed by the term:

$$\sigma_y = \frac{K_I}{\sqrt{2\pi r}} \qquad (2.1)$$

Here K_I is the stress intensity factor and r is the distance from the crack.
If at some distance $r=a_y$ from the crack tip the stress σ_y equals the yield stress f_y we have according to (2.1):

$$a_y = \frac{1}{2\pi}\frac{K_I^2}{f_y^2} \tag{2.2}$$

The stress resultant of the σ_y-stresses per unit thickness along the distance a_y is

$$\int_0^{a_y} \frac{K_I}{\sqrt{2\pi r}}\,dr = \sqrt{\frac{2}{\pi}}\,K_I\sqrt{a_y} = \frac{1}{\pi}\frac{K_I^2}{f_y} \tag{2.3}$$

This is twice the value of the resultant of the constant stress f_y along a_y.
This led Irwin **[60.2]** to suggest, that a plastic zone in the crack tip must have a length of $2a_y$. Half this length he considered as an additional crack length, which must be added to the real crack length a.
The additional term:

$$l_e = a_y = \frac{1}{2\pi}\frac{K_I^2}{f_y^2}. \tag{2.4}$$

is called the effective crack length term. The effective crack length then is:

$$a_{eff} = a + l_e \tag{2.5}$$

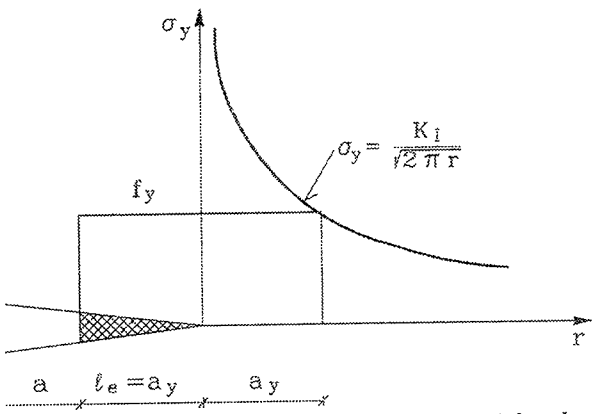

Figure 2.1 *Effective crack length at a crack tip with plastic yielding*

In **[90.1]** l_e has been determined in an alternative way by some approximate energy considerations.
For a material with yield strength f_y and tensile strength f_t it was shown that l_e may be put equal to:

$$l_e = a_p' = \frac{1}{2\pi}\frac{K_I^2}{f_y f_t} \qquad \textbf{(2.6)}$$

where a_p' is the length of the fracture zone, see figure 2.2. The length of the plastic zone a_y may be calculated by formula (2.2).

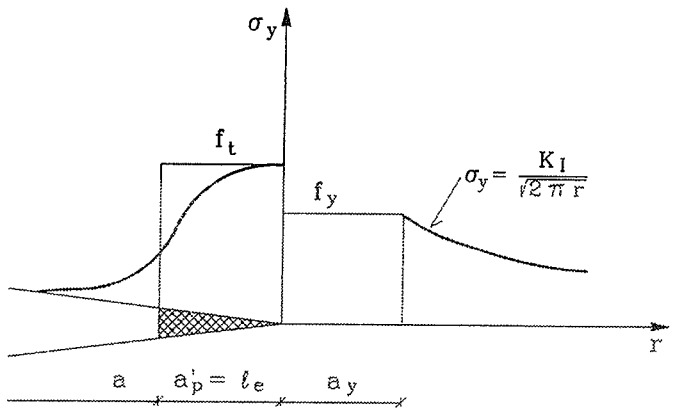

Figure 2.2 *Stresses at a crack tip*

2.3 The crack propagation formula

In this section the *energy crack propagation formula* will be presented. The formula is based on an energy criterion, which was introduced into the theory of cracks by Griffith **[21.1]**.

For a load controlled test, where the crack length a and the load P are the independent variables, the energy balance equation may be written, see **[90.1]**:

$$\frac{\partial W}{\partial a}da - P\frac{\partial u}{\partial a}da + G_F b da = 0 \qquad (2.7)$$

Here W is the elastic energy, u is the displacement in the direction of the load, G_F is the fracture energy and b is the thickness.

Taking the correction of the crack length l_e into account we get:

$$\frac{\partial W}{\partial a}da + \frac{\partial W}{\partial a}dl_e - P\frac{\partial u}{\partial a}da - P\frac{\partial u}{\partial a}dl_e + G_F b da = 0 \qquad (2.8)$$

which can be rearranged into:

$$(G_F b + \frac{\partial W}{\partial a} - P\frac{\partial u}{\partial a})da = -(\frac{\partial W}{\partial a} - P\frac{\partial u}{\partial a})dl_e \qquad (2.9)$$

By isolating da in (2.9) we get:

$$da = \frac{-\frac{\partial}{\partial a}(W - Pu)dl_e}{G_F b + \frac{\partial}{\partial a}(W - Pu)} \tag{2.10}$$

For a linear elastic body the potential energy W-Pu equals the elastic energy W with opposite sign in an equilibrium situation. Therefore:

$$\frac{\partial W}{\partial a} = \frac{\partial (Pu - W)}{\partial a} \tag{2.11}$$

Using this we get:

$$da = \frac{\frac{\partial W}{\partial a} dl_e}{G_F b - \frac{\partial W}{\partial a}} \tag{2.12}$$

In the symmetrical case, meaning a crack with two tips and the crack length defined as 2a, we have:

$$da = \frac{\frac{\partial W}{\partial a} dl_e}{2G_F b - \frac{\partial W}{\partial a}} \tag{2.13}$$

W still being the total elastic energy.
Since the crack length correction l_e depends on a as well as P we have:

$$dl_e = \frac{\partial l_e}{\partial P} dP + \frac{\partial l_e}{\partial a} da \tag{2.14}$$

which inserted into (2.12) gives:

$$da = \frac{\frac{\partial W}{\partial a}\left(\frac{\partial l_e}{\partial P}dP + \frac{\partial l_e}{\partial a}da\right)}{G_F b - \frac{\partial W}{\partial a}} \tag{2.15}$$

With a few rearrangements this leads to:

$$\frac{da}{dP} = \frac{\frac{\partial W}{\partial a}\frac{\partial l_e}{\partial P}}{G_F b - \frac{\partial W}{\partial a}\left(1 + \frac{\partial l_e}{\partial a}\right)} \tag{2.16}$$

The derivative $\partial W/\partial a$ should be taken at $a+l_e$, while $\partial l_e/\partial P$ and $\partial l_e/\partial a$ may be taken in a. The term $1+\partial l_e/\partial a$ is normally close to 1, whereby we get:

$$\frac{da}{dP} = \frac{\frac{\partial W_{(a+l_e)}}{\partial a}\frac{\partial l_{e(a)}}{\partial P}}{G_F b - \frac{\partial W_{(a+l_e)}}{\partial a}} \tag{2.17}$$

The change in the elastic energy may be expressed by the stress intensity factor K_I as (see **[86.1]**):

$$\frac{\partial W}{\partial a} = \frac{K_I^2}{E} \cdot b \tag{2.18}$$

and the fracture energy is defined as:

$$G_F = \frac{K_{IC}^2}{E} \tag{2.19}$$

K_{IC} being the critical value of the stress intensity factor.
In the symmetrical case we get:

$$\frac{\partial W}{\partial a} = 2\frac{K_I^2}{E}\cdot b \tag{2.20}$$

If (2.18) and (2.19) is inserted in (2.17) we get a formula using stress intensity factors:

$$\frac{da}{dP} = \frac{K_{I(a+l_e)}^2 \frac{\partial l_{e(a)}}{\partial P}}{K_{IC}^2 - K_{I(a+l_e)}^2} \tag{2.21}$$

In the symmetrical case we have, according to (2.13) and (2.20):

$$\frac{da}{dP} = \frac{K_{I(a+l_e)}^2 \frac{\partial l_{e(a)}}{\partial P}}{K_{IC}^2 - K_{I(a+l_e)}^2} \tag{2.22}$$

Notice that the formulas for the non-symmetrical and the symmetrical case are identical, when expressed by stress intensity factors.
By inserting the expression for l_e, (2.6), we get:

$$\frac{da}{dP} = \frac{K_{I(a+l_e)}^2 \frac{\partial}{\partial P}\left(\frac{K_{I(a)}^2}{2\pi f_y f_t}\right)}{K_{IC}^2 - K_{I(a+l_e)}^2} \tag{2.23}$$

This expression is called the *energy crack propagation formula* and by integration over one cycle the crack-velocity *da/dN* may be found as a function of P.

In a displacement controlled test we take the displacement **u** and the crack length **a** as the independent parameters. The energy criterion will then be:

$$\frac{\partial W}{\partial a}da + G_F b da = 0 \tag{2.24}$$

By using the same procedure as above we find the crack growth formula:

$$\frac{da}{du} = \frac{-\frac{\partial W}{\partial a}\frac{\partial l_e}{\partial u}}{G_F b + \frac{\partial W}{\partial a}(1 + \frac{\partial l_e}{\partial a})} \tag{2.25}$$

W is still the elastic strain energy, now being a function of a and u. It may be shown that:

$$\left(-\frac{\partial W}{\partial a}\right)_{P=const} = \left(\frac{\partial W}{\partial a}\right)_{u=const} \tag{2.26}$$

so in this case, (2.18) is replaced by:

$$\frac{\partial W}{\partial a} = -\frac{K_I^2}{E}\cdot b \tag{2.27}$$

Hereby a formula corresponding to (2.23) may easily be written down:

$$\frac{da}{du} = \frac{K_{I(a+l_e)}^2 \frac{\partial}{\partial u}\left(\frac{K_{I(a)}^2}{2\pi f_y f_t}\right)}{K_{IC}^2 - K_{I(a+l_e)}^2} \tag{2.28}$$

In this case the stress intensity factors must be determined as a function of **u** and **a**.

As shown in **[94.1]** the critical value of the stress intensity factor K_{IC} is not a constant, but very dependent of the stress intensity level K_I. The physical explanation is not yet fully understood, but tests have often shown increasing K_{IC} for increasing K_I, see i.e. **[70.1]**. The relation between K_{IC} and K_I may be written:

$$K_{IC} = M' K_I^{n'} \tag{2.29}$$

where M' and n' are empirical constants. This expression is inserted in formula (2.23) and (2.28) respectively.
M' and n' can be determined by tests as done in **[94.1]** or they can be estimated by the following equations:

$$\begin{aligned} n' &= 2 - \frac{1}{2}m \\ M' &= \frac{K_{IC}}{K_{IC}^{n'}} \end{aligned} \tag{2.30}$$

Here m is the exponent in the Paris equation:

$$\frac{da}{dN} = C \Delta K_I^m \tag{2.31}$$

and K_{IC} is the critical stress intensity factor. For more details about the K_{IC} dependency on K_I, see **[90.1]** or **[94.1]**.

It is well known that the crack growth rate depends upon the stress ratio $R = \sigma_{min}/\sigma_{max}$. The dependency is very clear close to the threshold value K_{th}, where crack propagation may start, and close to failure. In the middle region (Paris region II) the effect is most clear for a stress ratio R<0. When the stress ratio is larger than zero. meaning the specimen being in pure tension, the stress ratio effect is not very pronounced. In fact for steel it is often found that the crack growth rate is almost independent of R when depicted as a function of ΔK_I, see e.g. **[89.2]**. We define the stress range as $\Delta K_I = K_{Imax} - K_{Imin} = K_{Imax}(1-R)$. The influence from the R-ratio is illustrated in figure 2.3 for R > 0, showing the crack growth as a function of K_{Imax} and ΔK_I respectively.

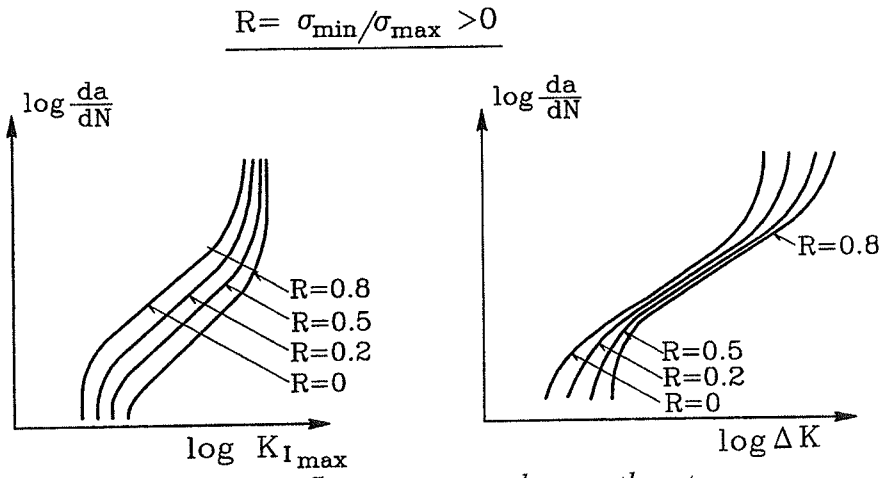

Figure 2.3 *R-ratio influence on crack growth rate.*

Several attempts to estimate the influence from the stress ratio, R, may be found in the literature.

Forman **[67.1]** suggested a correction of the order $(1\text{-}R)^{-1}$ related to ΔK_I, which corresponds to $\eta=(1\text{-}R)^3$ for Paris m=4 when related to K_{Imax}. Forman's formula to determine the crack growth rate may be written:

$$\frac{da}{dN} = \frac{C\Delta K_I^{\,n}}{(1-R)K_{IC}-\Delta K_I} \tag{2.32}$$

Nielsen **[90.1]** suggested a correction factor η, on the crack growth rate as a function of K_{Imax}, defined by

$$\eta = 1 - \frac{4}{3}R + \frac{1}{3}R^4$$
$$\frac{da}{dN}(R,K_{Imax}) = \eta\frac{da}{dN}(K_{Imax}) \tag{2.33}$$

Both corrections seem to give good results, when compared with some test results, but not in all cases, see **[89.2]**. The reason may be that the crack growth rate is almost independent of the stress ratio for R>0, when depicted as a function of ΔK_I. In the following a more accurate stress ratio correction factor will be derived.

Assuming the stress intensity factor K_I being far below the critical stress intensity factor, i.e $K_I << K_{IC}$, the term K_I^2 in the denominator in formula (2.23) may be neglected. Then we get:

$$\frac{da}{dP} = \frac{K_{I(a)}^2 \frac{\partial}{\partial P}\left(\frac{K_{I(a)}^2}{2\pi f_y f_t}\right)}{K_{IC}^2} \tag{2.34}$$

having further taken K_I in a instead of in $a + l_e$, which is reasonable because $a >> l_e$. Substituting the relation (2.29) into (2.34) it may be shown (see **[90.1,p50-52]**), that this equation may be written:

$$\frac{da}{dN} = \frac{1}{4\pi f_y f_t (M')^2} K_I^{4-2n'} \tag{2.35}$$

where K_I is equal to K_{Imax} for R=0.
Transforming this result from a function of K_{Imax} to a function of ΔK_I, demanding that the crack growth rate must be independent of R we get the equation:

$$\begin{aligned} \frac{1}{4\pi f_y f_t (M')^2} \Delta K_I^{4-2n'} &= \eta \frac{1}{4\pi f_y f_t (M')^2} K_{Imax}^{4-2n'} \\ &\Updownarrow \\ \Delta K_I^{4-2n'} &= \eta K_{Imax}^{4-2n'} \\ &\Updownarrow \\ \eta &= (1-R)^{4-2n'} \end{aligned} \tag{2.36}$$

This correction factor η ensures independence of R. For a material with a Paris m value of 3, meaning n'=0.5 see formula (2.30), we get the same result as Forman's formula. For crack growth rates with $m \neq 3$ we get another dependency, which still ensures independence of R, when da/dN is depicted as a function of ΔK_I.
It will be shown later in this paper that this correction factor gives extremely good results in comparison with the Forman equation for the materials treated. However, much more work must be carried out, before it can be concluded, that this is the correct way to take the stress ratio R into account.

When solving the crack propagation formula for $R \neq 0$, we integrate from K_{Imin} to K_{Imax}. The influence from K_{Imin} is very small, due to the fact that for instance for Paris m=4 we have $K_{Imax}^4 >> K_{Imin}^4$.

A phenomenon which may be of value when explaining the R-dependency on the crack growth rate is crack closure. Crack closure is illustrated in figure 2.4. Because of the plastic deformations the crack will close during unloading before the specimen is totally unloaded. Since the crack is open only for a part of the loading sequence an effective stress intensity factor range $\Delta K_{eff} = K_{Imax} - K_{op}$ is governing the crack growth, K_{op} being the stress intensity factor when the crack starts to open and the crack starts to propagate. This explains the delay of crack propagation caused by overloading. Furthermore the crack propagation is delayed in general and should to some degree be a function of ΔK_{eff} instead of ΔK_I. If the R ratio is high the effect will be reduced, because K_{Imin} approaches K_{op} and the effective stress range ΔK_{eff} equals ΔK_I.

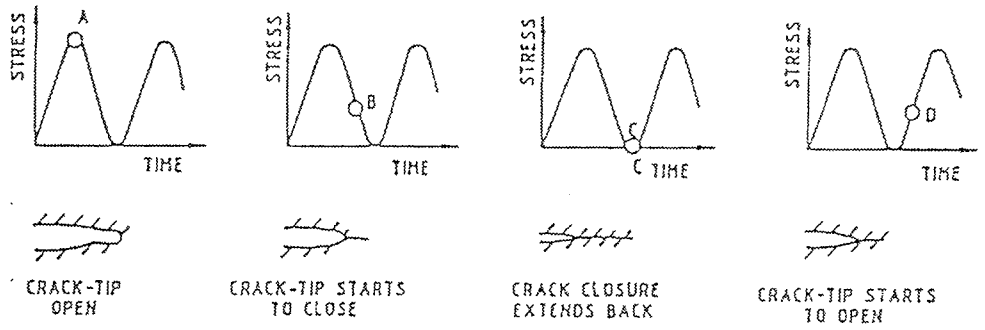

Figure 2.4 *Crack opening and crack closure*

Elber [71.2] was the first to observe this phenomenon. He suggested the simple relation:

$$\Delta K_{eff} = (0.5 + 0.4R)\Delta K_I \qquad (2.37)$$

where ΔK_{eff} should be used in the crack propagation formulas, like the Paris formula, i.e.

$$\frac{da}{dN} = C\Delta K_{eff}^{m} \qquad (2.38)$$

In **[71.2]** it was shown that for Al2024-T3 similar curves were obtained when applying (2.38) for different R ratios and depicting the result in a ΔK_I-da/dN diagram. However it is known that for many materials, especially steel, the same ΔK_I-da/dN curve is obtained for different values of R, see figure 2.3. This is valid for both of the test series treated in this paper. Therefore equation (2.36) can not be applied for steel in general. A more accurate equation must be developed, probably depending on the shape and size of the plastic zone, and based on actual measurements of the crack closure behaviour for the actual material treated.
A large investigation of crack closure has been carried out by Ibsø **[95.1]** on the specimens investigated in this paper. The model to determine the effect of crack closure was based on the determination of a crack opening stress S_o. The crack opening stress intensity factor K_{op} then was determined by

$$K_{op} = \beta S_o \sqrt{\pi a} \qquad (2.39)$$

Neglecting the influence from the residual stresses in the specimens, it was found that the crack opening stress S_o equals about $0.3 \cdot \sigma_{max}$ for R=0. A plane strain constraint factor of about 2.4 was used. This factor takes into account the increased yield strength at the crack tip in plane strain conditions. In plane stress $S_o \approx 0.5 \cdot \sigma_{max}$.
The residual stress field will increase the crack opening stress S_o. The residual stress field may be considered as an increase in the relative stress level, which means that the actual maximum stress equals $\sigma_{max}+\sigma^{yy}_r$, where σ^{yy}_r is the value of the residual stress. Applying this assumption the crack opening stress may be approximately determined by the equation:

$$S_o = 0.3 \cdot (\sigma_{max} + \sigma_r^{yy}) \qquad (2.40)$$

The equation (2.40) will be used in section 5.3 to determine the effect of crack closure including the effect from the residual stress field.

Chapter 3

Basic problems and concepts

3.1 Introduction

In this chapter some basic problems in fatigue of welded structures will be shortly presented. This includes a discussion of stress intensity factors for welded connections, crack growth in welded connections, the S-N diagram (Wöhler curve) and some discussion of residual stresses. The subjects mentioned will be presented in section 3.2. In section 3.3 the crack propagation formula will be further developed, so it can be used to calculate the S-N diagram for welded connections.

3.2 Welded connections in general

All structures have defects, either built in during fabrication or initiated by the service conditions of the structure. These defects will develop to cracks and if the structure is subjected to fatigue loading, the cracks will propagate. Welded connections normally have manufactured defects in the material, which under the right loading conditions lead to fatigue crack propagation. A measure of the severity of the crack propagation is given by the stress intensity factor, K_I, which describes the intensity of the stress field in a small region surrounding the crack tip, cf section 2.2. The rate of crack propagation is a function of the range of the stress intensity factor, ΔK_I. It is therefore necessary to compute the stress intensity factor. In this report two cases will be of special interest and will be introduced in the following. In the case of welded joints, see figure 3.1, the stress intensity factor is determined by the general equation (3.1), see for instance **[77.2]** and **[85.1]**.

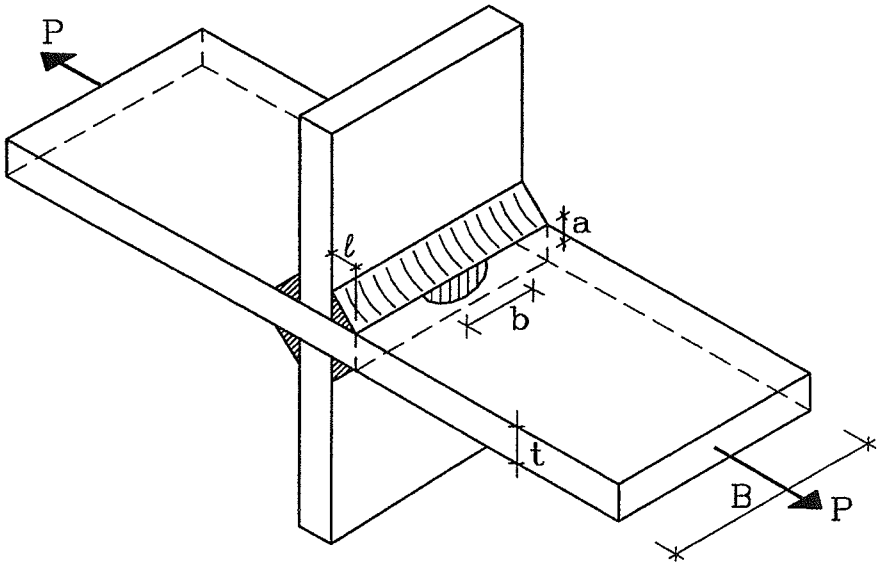

Figure 3.1 *Welded Joint Test specimen.*

$$K_I = F_S \cdot F_E \cdot F_G \cdot F_T \cdot \sigma\sqrt{\pi a} \tag{3.1}$$

where
- F_S Correction factor for free surface.
- F_E Correction factor for crack shape.
- F_T Correction factor for finite thickness or finite width.
- F_G Geometry correction factor accounting for the effect of stress concentration due to geometrical discontinuity.

The correction factors in formula (3.1) can be expressed as follows:

$$\begin{aligned} F_S &= 1.12 - 0.12\frac{a}{b} \\ F_E &= \left[1 + 4.5945\left(\frac{a}{2b}\right)^{1.65}\right]^{-\frac{1}{2}} \\ F_T &= \sqrt{\sec(\pi a/2t)} \end{aligned} \tag{3.2}$$

The crack, see figure 3.1, is assumed to have elliptical shape.

The elliptical crack shape ratio a/b is normally in the range 0.2 to 0.5. In section 4.3 it is observed that the specimens examined in this work have an elliptical shape ratio of about a/b = 0.25.

The geometrical correction factor F_G has been approximatly determined in **[90.2]** by using a method suggested by Albrecht **[77.2]**. The values are listed in appendix B. An approximate analytical expression suggested in **[85.1,pp.119]** for non-load carrying fillet welded joints will be used:

$$F_G = \frac{SCF}{1 + \frac{1}{d}\left(\frac{a}{t}\right)^q} \qquad (3.3)$$

where:
F_G = the geometrical stress gradient correction factor
SCF = elastic stress concentration factor at the weld toe
a = crack length.
t = thickness.
d = stress gradient correction factor decay coefficient.
q = stress gradient correction factor decay exponent.

The elastic stress concentration factor SCF can approximately be determined by the formula:

$$SCF = 1.621 \cdot \log\left(\frac{l}{t}\right) + 3.963 \qquad (3.4)$$

for a non-load carrying fillet weld connection, l being the width of the weld toe, see figure 3.1.
The constants d and q in formula (3.3) will be estimated on the basis of a FEM calculation, see appendix B, and compared with values normally used, see section 5.3.

In the case of welded CCT specimen, see figure 3.2, the stress intensity factor is determined by the general equation (3.5), see **[79.1]** or **[66.1]**.

$$K_I = \sigma\sqrt{a}\left[1.77+0.277\left(\frac{2a}{W}\right) -0.51\left(\frac{2a}{W}\right)^2+2.7\left(\frac{2a}{W}\right)^3\right] \tag{3.5}$$

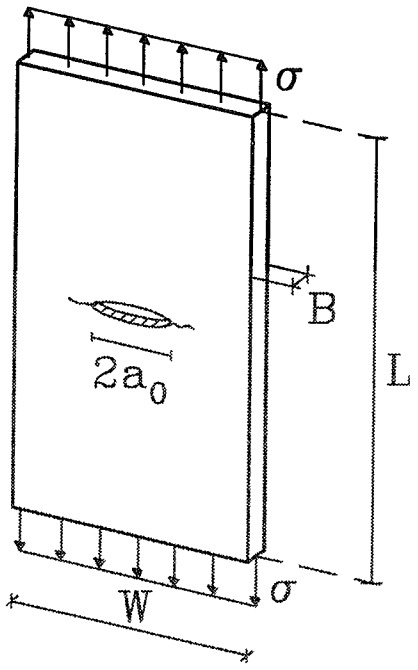

Figure 3.2 *Center Cracked Test specimen.*

Normally two methods are used to present crack propagation results. These are the da/dN-ΔK_I curve and the S-N curve. The da/dN-ΔK_I-curve shows the whole range of the crack propagation rate from region I: threshold (initiation of crack) through region II: the Paris area (stable crack growth) to region III: critical stress intensity range (unstable crack growth), see figure 3.3.

In some tests it is not possible to measure the crack length with sufficient accuracy during crack growth. In such cases it will not be possible to determine the ΔK_I and the da/dN curve can not be produced. This is normally the case for welded joints, due to the fact that the crack propagates elliptically into the material as shown in figure 3.1. In this case only the number of cycles to failure $\mathbf{N_f}$ is measured for varying stress levels $\Delta\sigma$.

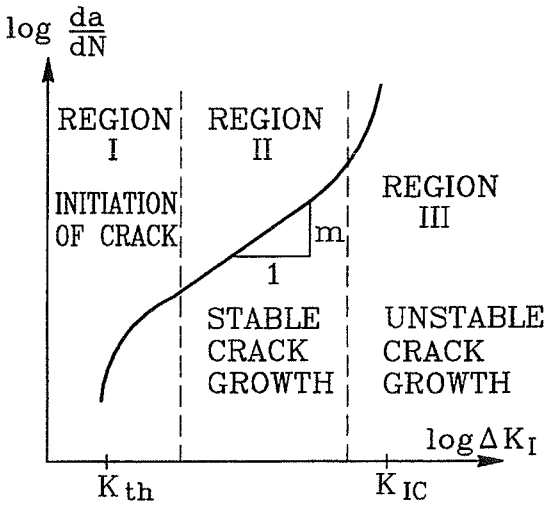

Figure 3.3 *da/dN-ΔK_I - curve.*

The total number of cycles to failure is subdivided into two phases. The first phase is the initiation period with no crack growth, the second one the crack propagation phase, se figure 3.3. The number of cycles in the two phases are denoted $\mathbf{N_i}$ and $\mathbf{N_p}$ respectively.

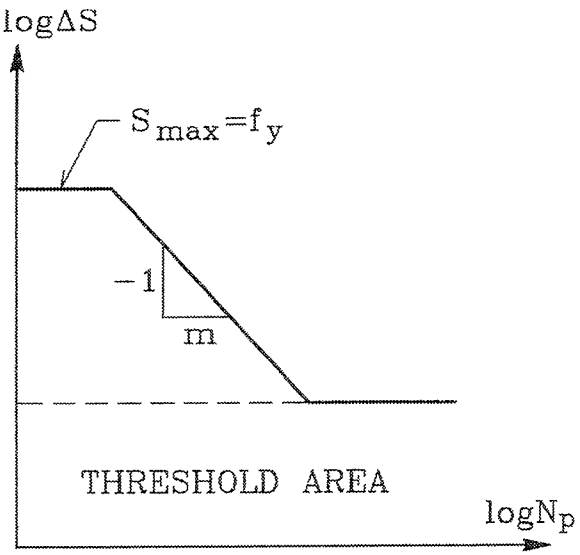

Figure 3.4 *S-N diagram.*

If we depict the stress range ΔS as a function of the number of cycles N_p in a double logarithmic diagram we get the S-N curve shown in figure 3.4.

If the stress level is lower than a certain value the crack will never initiate. meaning that the stress intensity is lower than the threshold value. This results in a horizontal line in the S-N curve. Likewise an upper limit exists which equals the stress level for a pure statical yield failure of the material, see figure 3.4. The S-N curve is often used in practice to estimate the fatigue service failure of a structure.

In the following the effect of residual stresses on crack growth will be discussed. Residual stresses may be defined as a selfequilibrated stress field existing in a body without any externally applied load. Residual stresses may be produced by a previous overload in a fatigue process producing plastic strains or by a heating process, for instance from welding, where the temperature distribution in the body is far from uniform, and the thermal stresses produce plastic deformations. After cooling, the plastic deformations remains and a residual stress field is formed. A third example of residual stresses may be due to pure compression on a certain area of the body produced by peening, a cold-working process, where compressive residual stresses are introduced in the surface layer by battering the specimen with a high velocity stream of metal particles.
When treating welded joints we have to take into account the effect of residual stresses introduced in the specimens.
A residual stress field in a cracked body will normally be of the form shown in figure 3.5:

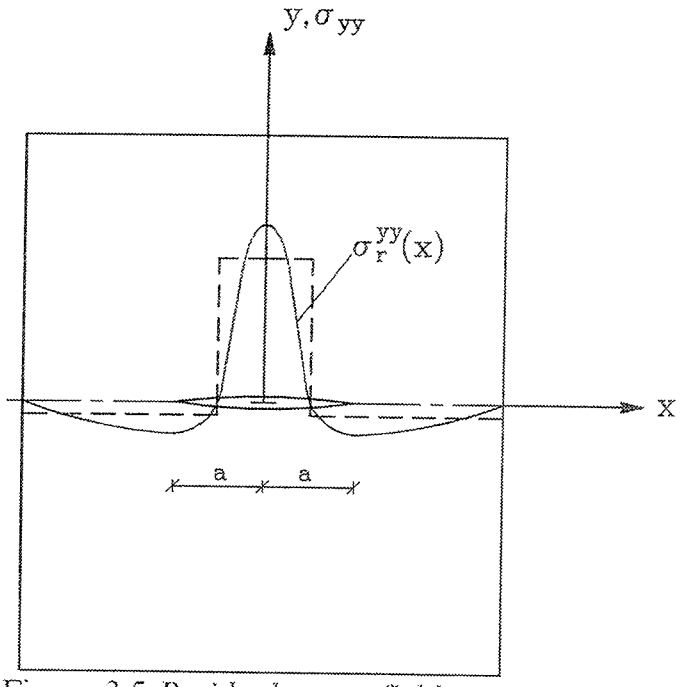

Figure 3.5 *Residual stress field.*

Most frequently the method used to take into account the effect of residual stresses on crack growth utilizes the superposition principle of the stress intensity factor, i.e superposition of the stress intensity factors of the applied load and the residual stresses respectively, see e.g. **[89.1]**.

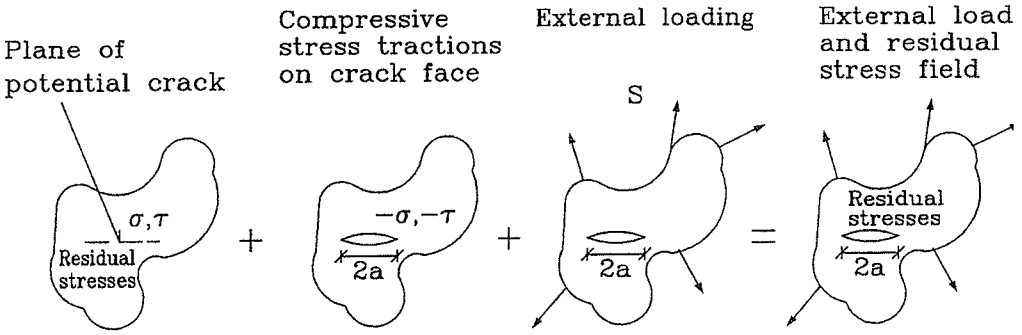

a) $K=0$ b) $K=K_r$ c) $K=K_s$ d) $K=K_r+K_s$

Figure 3.6 *Superposition of stress intensity factors.*

When a crack is introduced in a body, there will be a redistribution of the stresses and the stress intensity factors may be calculated using the superposition principle illustrated in figure 3.6.

The stress intensity factor K_r due to the residual stress fields may be computed by using e.g. the weight function approach given by Büeckner **[71.1]**, Greens function **[82.1]** or existing numerical methods. Several solutions have been developed for practical applications, see e.g. **[73.1]** or **[76.1]**.

In general, the stress intensity factor K_r is determined by the expression shown in formula (3.6):

$$K_r = \int_{-a}^{a} \sigma_r^{yy}(x)\, h(x)\, dx \qquad (3.6)$$

where σ_r^{yy} is the residual stress field, h(x) the weight function describing the influence of the crack, and a is half the crack length in a symmetrically cracked body. If we as an example consider an infinite body with a center crack as shown in figure 3.5 the weight function will be, see e.g. **[86.1]**:

$$h(x) = \frac{1}{\sqrt{\pi a}}\sqrt{\frac{a-x}{a+x}} \tag{3.7}$$

Inserting into formula 3.6 we get:

$$K_I = \sqrt{\frac{1}{\pi a}}\int_{-a}^{a} \sigma_r^{yy}(x)\sqrt{\frac{a-x}{a+x}}dx \tag{3.8}$$

which in the case of a symmetrical stress distribution can be rearranged to:

$$K_I = \sqrt{\frac{1}{\pi a}}\int_{0}^{a} \sigma_r^{yy}(x)\left[\sqrt{\frac{a-x}{a+x}}+\sqrt{\frac{a+x}{a-x}}\right]dx \tag{3.9}$$

From this formula we find the following stress intensity factor which takes into account the residual stress field σ_r^{yy}:

$$K_I = 2\sqrt{\frac{a}{\pi}}\int_{0}^{a} \frac{\sigma_r^{yy}(x)}{\sqrt{a^2-x^2}}dx \tag{3.10}$$

In the special case where the residual stress field is constant, i.e $\sigma_r^{yy}=\sigma=$const, we get the solution:

$$K_I = \sigma\sqrt{\pi a} \tag{3.11}$$

This formula will be used here when determining the effect of residual stresses on crack growth.
In practice the body is a finite plate. General solutions of weight functions may be derived from the infinite case using the superposition principle, leading to a formula of the type:

$$K_I = \beta\sigma\sqrt{\pi a} \tag{3.12}$$

where β is a geometrical correction factor taking into account the finite dimensions.

By superposition the final value of K_I is determined by the stress intensity factor from the external load, K_s, and the stress intensity factor K_r accounting for the residual stresses:

$$K_I = K_s + \sum_{a_i=a_1}^{a_n} K_r \qquad (3.13)$$

Here K_s is from the external load, K_r is determined by formula (3.10), for a number of constant residual stress fields along the crack length intervals a_i and β is the correction factor, see formulas (3.1), (3.5) and (3.12). This procedure rests on the assumption that a residual stress field may be approximated by a series of constant stress fields satisfying the equilibrium conditions as illustrated with the dashed line in figure 3.5. The error by doing this is normally negligible if the specimen is in pure tension, but in the case of compression it is necessary to use the original residual stress field and solve equation (3.8).

The residual stress field σ_r^{yy} from welding or introduced by peening etc. can be determined experimentally by several methods, e.g. the hole-drilling technique, X-ray measurements or strain measurements, see **[89.2]**. Normally strain measurements using strain gauges are used. In chapter 4 the residual stress fields measured in the two test series treated in this work are presented.

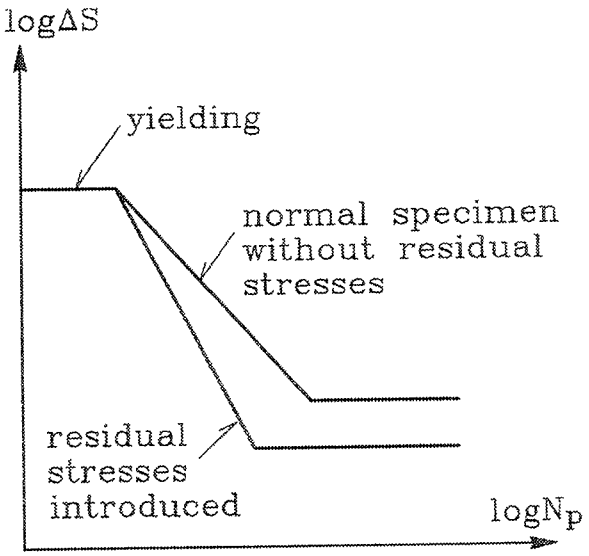

Figure 3.7 *Effect from residual stresses.*

Local residual stresses will in general be relaxed by cyclic loading if the total stress - applied plus residual - exceeds the yield stress. Residual stresses are therefore insignificant in the low life range of the S-N curves. In the long life range the residual stresses lead to a rotation of the S-N curve as illustrated in figure 3.7. In practice this rotation is rather small and may be considered as a material property, which is taken into account by the Paris m value, see formula (2.31).

3.3 Crack propagation formula applied to welded joints

The energy crack propagation formula gives the crack propagation velocity da/dP as a function of the actual crack length **a** and the stress intensity factor K_I, which in general form may be written:

$$K_I = \beta \cdot \sigma \sqrt{\pi a} \tag{3.14}$$

The parameter β depends on the geometry of the specimen, and is typically a function of the crack length **a** and the width (or thickness) **W**. If the crack propagation formula is solved by integrating over one cycle, having **P** as the controlling parameter, the crack propagation for one cycle, denoted **da/dN**, is found. Calculating the related stress intensity factor range ΔK_I, the da/dN-ΔK_I curve can easily be produced.
Thus the crack propagation formula gives the da/dN curve as a result. This can be used to calculate the S-N curve as will be demonstrated in the following. As mentioned in section 3.2, the S-N curve must be used when comparing with experiments on Welded Joint Test specimens if the crack length has not been measured. If the well-known Paris equation is used, we have

$$\frac{da}{dN} = C\Delta K_I^{\,m} \tag{3.15}$$

Inserting formula (3.14) and solving the simple differential equation we get the number of cycles to failure

$$N_p = \int_{a_i}^{a_f} \frac{1}{C(\beta \Delta \sigma \sqrt{\pi a})^m} da \tag{3.16}$$

where a_i is the crack length at initiation and a_f is the crack length at failure.
For constant amplitude loading the result simplifies to:

$$N_p = \frac{1}{C(\Delta \sigma)^m \pi^{m/2}} \int_{a_i}^{a_f} \frac{1}{\beta^m a^{m/2}} da \tag{3.17}$$

which can be rearranged to:

$$\Delta\sigma = \left(\frac{1}{C\pi^{m/2}} \int_{a_i}^{a_f} \frac{1}{\beta^m a^{m/2}} da \right)^{-\frac{1}{m}} \cdot N_p^{-\frac{1}{m}} \qquad \textbf{(3.18)}$$

Since the S-N curve gives the stress range $\Delta\sigma$ as a function of the number of cycles, it appears that the slope of the S-N curve may be used to estimate the m-value in Paris' equation.

When the energy crack propagation formula is used to predict the S-N curve a similar procedure may be used. If we write the result of the energy crack propagation formula in the form: $f(\Delta K_I)=da/dN$ determined by integrating equation (2.23) over one cycle, then by integrating numerically over the range a_i to a_f we may determine the number of cycles to failure by formula (3.19):

$$N_p = \int_{a_i}^{a_f} \frac{1}{f(\Delta K_I)} da \qquad \textbf{(3.19)}$$

The procedure used to solve the crack propagation problem consists of two numerical procedures. The crack propagation formula, see (2.23), can be solved for instance by using a fourth order Runge Kutta method. To solve equation (3.19) a simple numerical integration formula like the trapezoid formula can be used. In appendix C a pascal program to solve the routines is listed.

The parameter a_f is the critical crack length, which may be determined by means of K_{IC}. The results of equations (3.17) and (3.19) depends on the crack geometry. However the influence of a_f fortunately is insignificant if $a_f >> a_i$. Therefore a_f may be chosen arbitrarily to half the thickness of the specimen. This crack length corresponds to the final critical crack length observed in many fatigue tests, see **[95.1]**. It will be shown in chapter 5 that the effect of a change in a_f in this range is negligible.

On the contrary the initial crack length a_i has a large influence on the result. Therefore it is necessary to determine the initial crack length quite accurately. When manufacturing welded joint connections the base metal melts in the welding zone. This results in a small void between the weld metal and the base metal, see figure 3.8. This void represents the notch or the initial crack length a_i, which leads to crack propagation. The size of the initial crack length may be determined using

microscopic analysis of the tests specimens. A series of investigations have been performed and the conclusion is that the length is in the order of $a_i \approx 0.075$ mm to $a_i \approx 0.4$ mm, see **[89.1]**. The lower bound takes into account the fact that some irregularities at the weld toes will always exist. The upper bound is likely to be a limit of what is accepted before repairing of the weld toe is considered. In chapter 5 some parameter studies will be performed to illustrate the effect of the initial crack length. When comparing with test results the initial crack length will be put equal to $a_i = 0.2$ mm as a reasonable average value, which has often been used when analyzing non-load-carrying fillet welded joints.

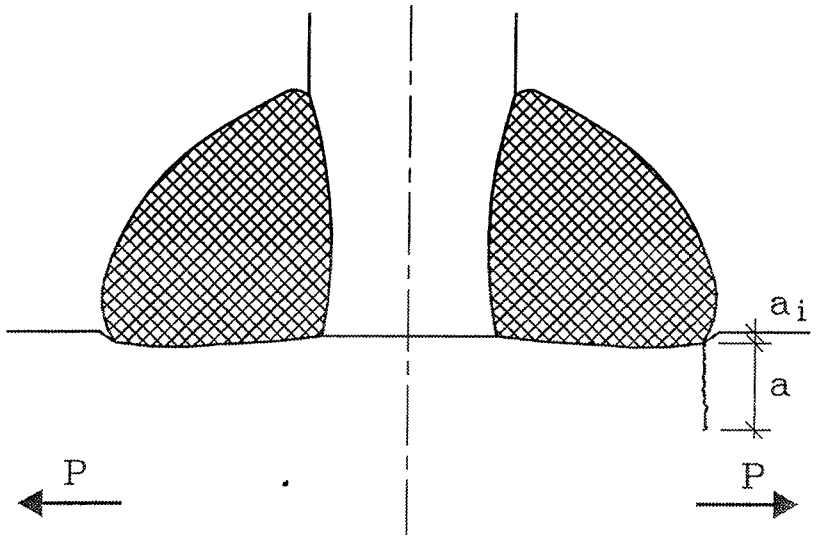

Figure 3.8 *Initial crack at weld toe.*

Chapter 4

Presentation of two test series on welded connections

4.1 Introduction

In this chapter two test series with welded connections are presented. In the next chapter the test results will be used to evaluate the crack propagation formula. The first test series (see section 4.2) is chosen because it very clearly shows how the crack velocity da/dN depends upon different types of welding connections in the plates. The test specimen is a standard Center Cracked Test specimen (CCT) welded together in different directions compared to the crack propagation direction. Only tests with constant amplitude loading will be examined. The tests were performed by Glinka **[79.1]**.

The second test series (see section 4.3) consists of a test series with welded joints between to plates. The test series has been chosen because such welded joint plates are very similar to those used in real structures, as for example off-shore structures. These connections are often suffering from severe fatigue fracture due to the lack of knowledge in fracture mechanics behaviour of welded connections. The crack propagates elliptically, starting at the weld toe and developing into the plate material. Therefore the crack propagation is very difficult to measure exactly. So in this case the purpose will be to predict the S-N curve using the crack propagation formula. The tests were performed by Ibsø **[92.1]**

4.2 Welded Center Cracked Test Specimens (WCCT)

These tests were made with the purpose to investigate the effect of residual stresses arising in welded connections. The problem will be discussed further in chapter 5. In the following the test results will be presented.
The tests were performed under constant and variable amplitude loading. However only the tests with constant amplitude loading will be presented in this paper.
All specimens, see figure 4.1, were made of one metal sheet 4 mm thick. The material was a low alloyed hot-rolled medium strength steel 18G2AV. The mechanical properties are shown in table 4.1. The tests were, as mentioned, performed by Glinka **[79.1]**.

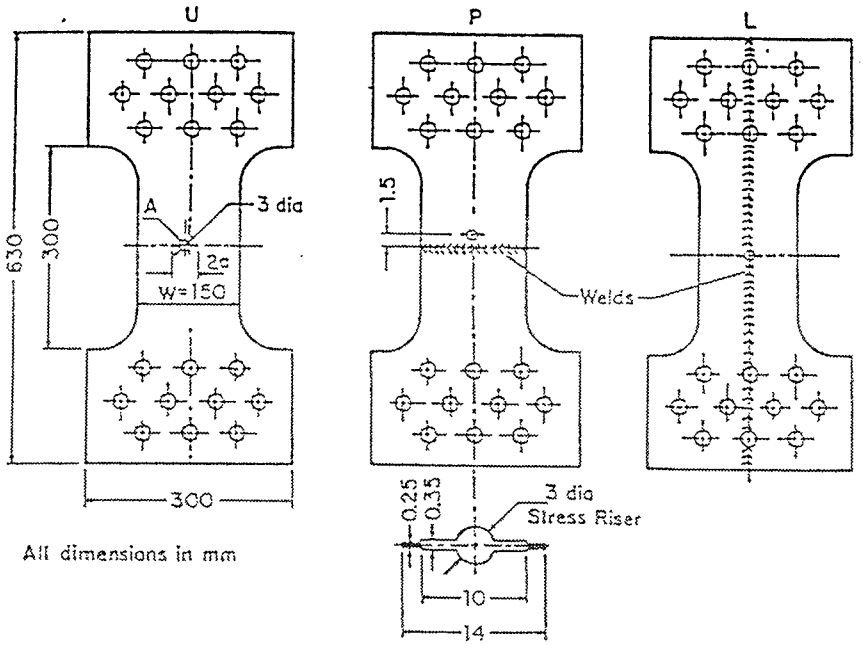

Figure 4.1 *Welded Center Cracked Test specimens (WCCT).*

18G2AV	
f_y (MPa)	f_u (MPa)
625	784

Table 4.1 *Mechanical properties*

The critical stress intensity factor K_{IC} was not measured. On the basis of the yield strength, and knowing that we are dealing with a normal graded steel, the critical stress intensity factor can be estimated to be about $K_{IC} \approx 120$ MN/m$^{3/2}$, see **[86.1]**. Furthermore ΔK_I at failure equals about 50 MN/m$^{3/2}$ for a stress ratio of R=0.5 which corresponds to a K_{IC} value higher than 100 MN/m$^{3/2}$, see figure 4.3.
The residual stress field due to the welding has to be taken into account when analyzing the data. In general we will always observe tension stresses close to the welded joint and compression in some distance from the joint.
The tensile residual stress field near the joint is mainly due to cooling of the weld attachment. When it cools down it will try to shorten leading to tension. Since residual stresses are selfequilibrating, we will get compression in some distance from the weld toe.
The residual stress field obtained by strain gauge measurements for specimen P, perpendicular welds, and for specimen L, longitudinal welds, is shown in figure 4.2, **[79.1]**. Due to symmetry only one half of the specimen is shown.

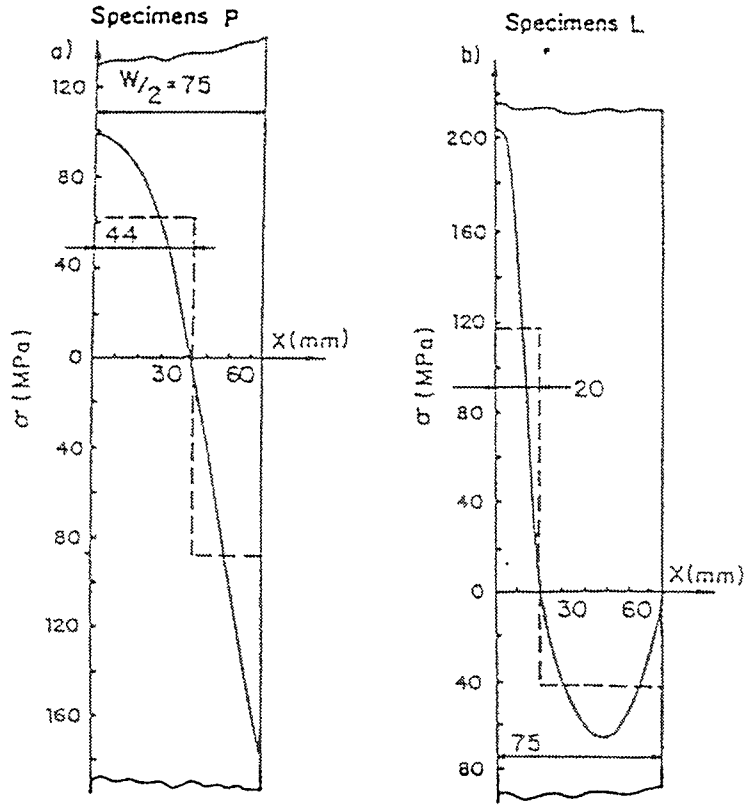

Figure 4.2 *Residual stress distribution in the plane of fatigue crack growth,* **[79.1]**.

As shown in figure 4.2, dashed lines, the residual stress field is approximated with two intervals of constant stress for each specimen, which is sufficiently accurate, when the specimens are loaded in pure tension, i.e. $R = \sigma_{min}/\sigma_{max} = 0$, see section 3.3. With the stresses shown in table 4.2 equilibrium is obtained.

	Specimen P		Specimen L	
crack interval	a=0-44 mm	a=44-75 mm	a=0-20 mm	a=20-75 mm
σ_r^{yy}	62 MPa	-88 MPa	118 MPa	-43 MPa

Table 4.2 *Residual stress distribution in specimens P and L.*

The specimens were cut out parallel to the rolling direction. In order to obtain similar residual stress distributions in each welded specimen, the specimens were welded after complete preparation of separate details.
Three different test specimens were made, see figure 4.1. The da/dN - ΔK_I relation is shown in the figures 4.3 to 4.5. The tests were performed with varying R ratio ($\sigma_{min}/\sigma_{max}$). The variation is small and does only effect the da/dN - ΔK_I behaviour very little, as shown in the figures. The small influence of the stress ratio R on the da/dN - ΔK_I curve is discussed in section 2.3.

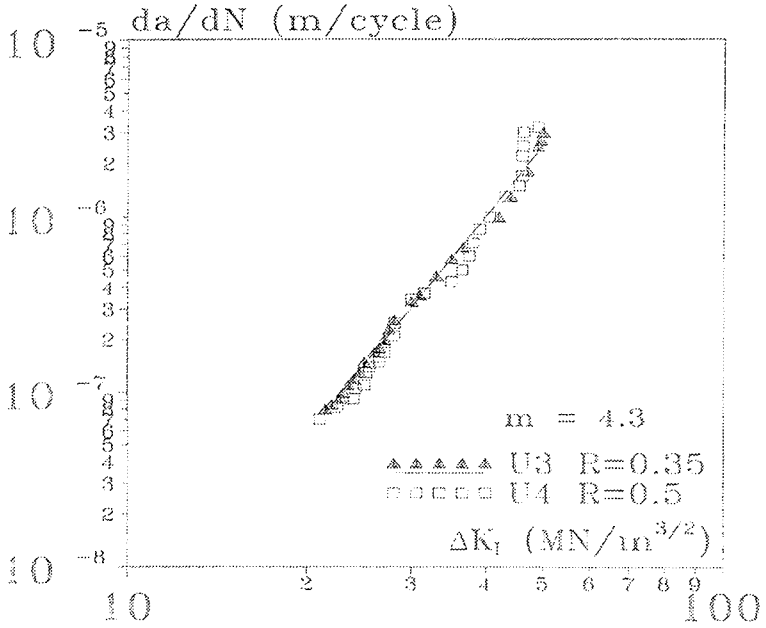

Figure 4.3

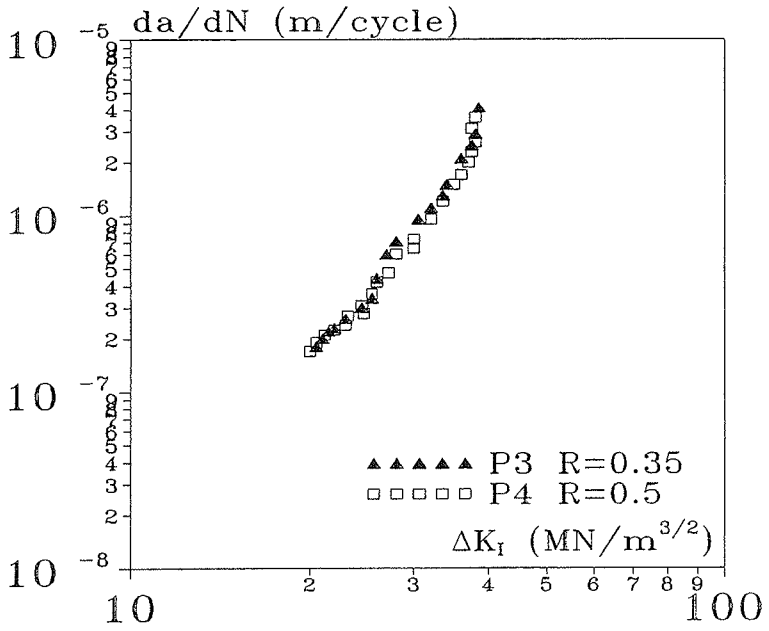

Figure 4.4

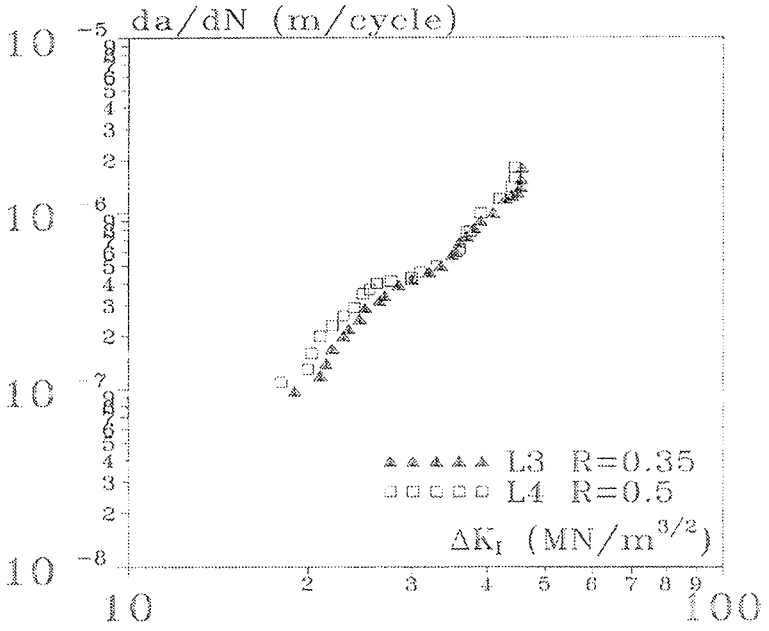

Figure 4.5

It is observed that the crack propagating rate depends on the type of the welded connection. If we combine the three curves, the effect is more clear. In figures 4.6 and 4.7 it is seen that the crack propagation rate is faster for specimens P (welded parallel to the crack direction) than for specimen U (not welded). For specimen L (welded perpendicular to the crack direction) it is observed that the crack propagation in the beginning follows specimen L, and in the end follows specimen U. In between there is a transition with a very slow crack propagation. In **[79.1]** the phenomenon is explained as an effect of residual stresses. In chapter 5 a method to model this will be presented.
The specimen U is considered as a reference specimen to the residual stress effect. In figure 4.3 it is observed that the Paris m value is equal to m=4.3. This value will be used when predicting the crack propagation in chapter 5.

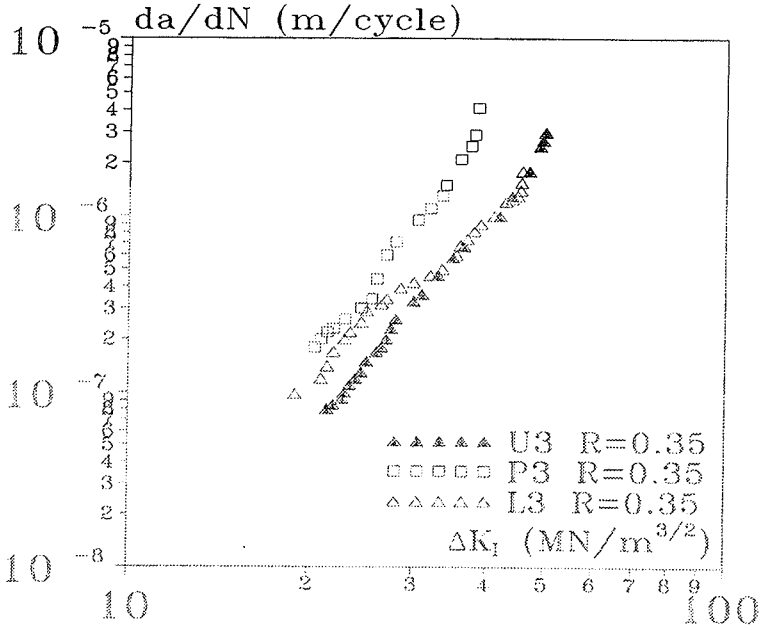

Figure 4.6

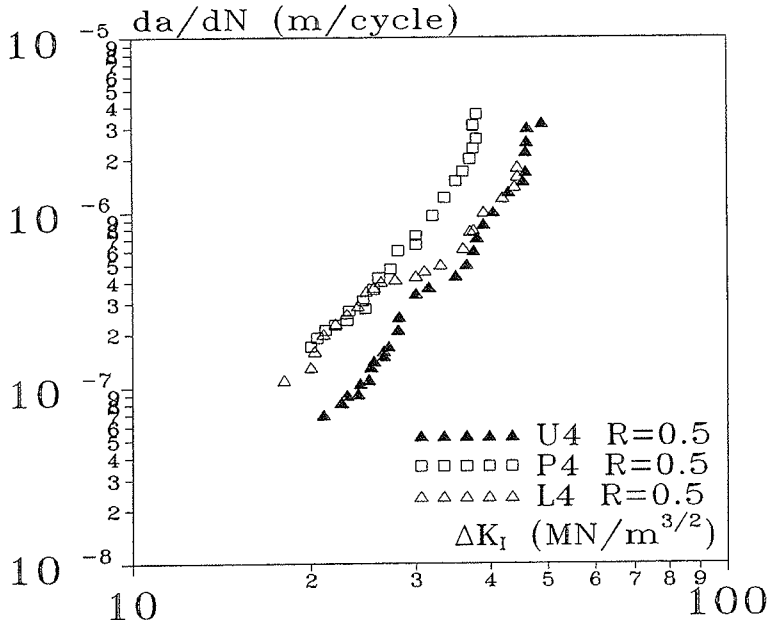

Figure 4.7

4.3 Welded Joint Test Specimens (WJT)

In this section the test results from the welded plates, shown in figure 4.8, will be presented. The tests were performed under constant amplitude loading.
Two specimen types were made, one metal plate 8 mm thick and one metal plate 16 mm thick. They were made by steel St. 52-3 (Fe 510C) according to DIN 17100. The tests were performed by Ibsø **[92.1]**.

Figure 4.8 *Welded Joint Test specimens (WJT),* **[92.1]**.

The measured mechanical properties for the steels used are listed in table 4.3:

	f_y MPa	f_u MPa	Elongation %
plate 16	409	575	25.9
plate 8	400	537	30

Table 4.3 *Mechanical properties from tensile tests*

In the test series with the welded joints, the critical stress intensity factor K_{IC} was not measured. In stead Charpy V-Notch (CVN) tests were performed, which may be used to estimate K_{IC}.

In table 4.4 the results from the CVN tests are shown.

Charpy V-Notch tests		
	Range [Nm]	Mean [Nm]
Plate 16	102-106	104
Plate 8	103-118	108

Table 4.4 *Charpy V-Notch test results.*

We observe from table 4.4 that CVN can be put equal to approximately 106 Nm. To estimate K_{IC} two methods will be used. In Barsom and Rolfe **[77.1, pp 177]** the empirical expression **(4.1)** is derived on the basis of tests with 11 different alloy steels with a yield strength in the range 760 to 1700 MPa (expression **(4.1)** is transformed from American units into SI units with f_y in MPa and K_{IC} in $MN/m^{3/2}$.)

$$\left(\frac{K_{IC}}{f_y}\right)^2 = 0.646\left(\frac{CVN}{f_y} - \frac{1}{100}\right) \qquad (4.1)$$

Having the yield strength $f_y \approx 405$ MPa and CVN $\approx$ 106 Nm we get from formula (4.1): $K_{IC} = 163$ $MN/m^{3/2}$.

Another method has been described in Broek **[86.1, pp 322]** where the relation between K_{IC} and CVN is related to the modulus of elasticity. The empirical formula is based on tests with 9 different alloy steels. There is a larger scatter in these

results, but they can still be used to give a good estimate of the K_{IC} value. A linear fit gives the expression (4.2):

$$\frac{K_{IC}^2}{E} = 1.722 \cdot 10^{-3} \cdot CVN \qquad \textbf{(4.2)}$$

Having the modulus of elasticity E = 210000 MPa and CVN ≈ 106 Nm we get K_{IC} = 195 $MN/m^{3/2}$.
On basis of these two calculations the critical stress intensity factor may be estimated to be about $K_{IC} \approx 180$ $MN/m^{3/2}$, a quite realistic value for medium strength steel.

In figure 4.9 a fractured specimen is shown. We observe that the elliptically shaped crack front have a shape ratio of about a/b = 0.2. All test specimens had shape ratios within a/b = 0.2 and 0.3, see **[95.1]**. An average value of a/b=0.25 will be used in the calculations in section 5.3.

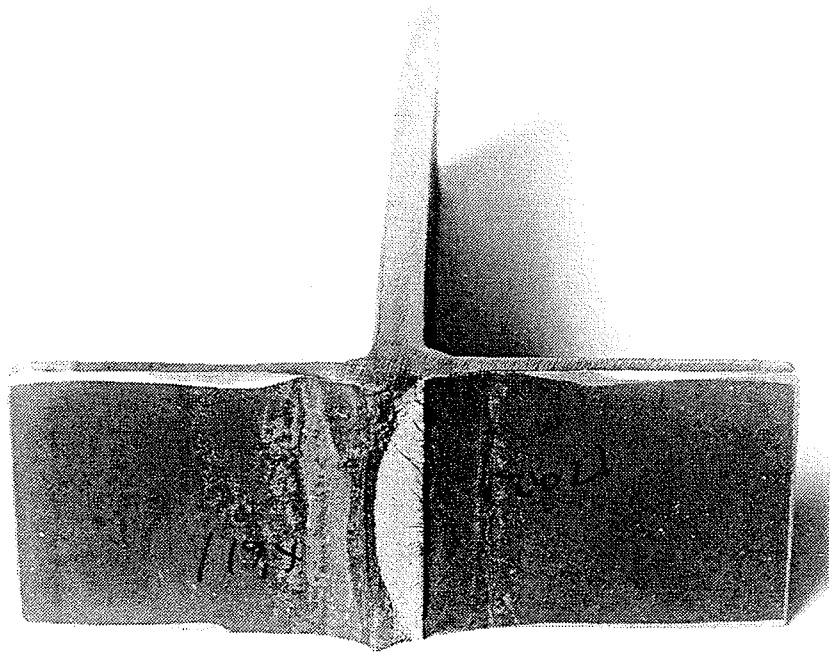

Figure 4.9 *WJT specimen at failure.*

The residual stress field due to the welding has to be taken into account when analyzing the data. In figure 4.10 and 4.11 the residual stresses measured with strain gauges are shown, **[95.1]**.

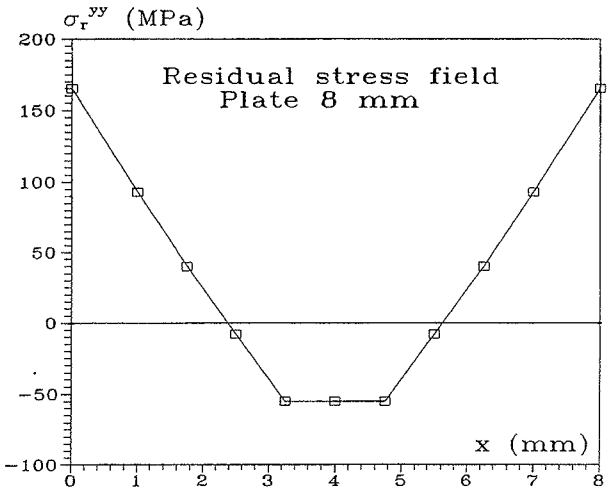

Figure 4.10 *Residual stress distribution in the plane of fatigue crack growth, plate 8 mm.*

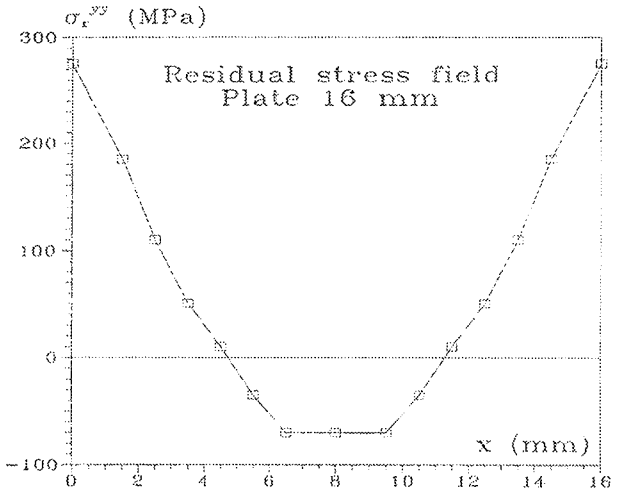

Figure 4.11 *Residual stress distribution in the plane of fatigue crack growth, plate 16 mm.*

The crack propagates from x=0 to half the specimen width. The specimen is pretensioned due to the residual stresses in the first part of the crack propagtion. After some crack growth the crack reaches the compression zone and the effect from the residual stresses will be reduced.
The test specimens were subjected to constant amplitude fatigue loading until failure. The results are presented in S-N diagrams, see figures 4.12 and 4.13.

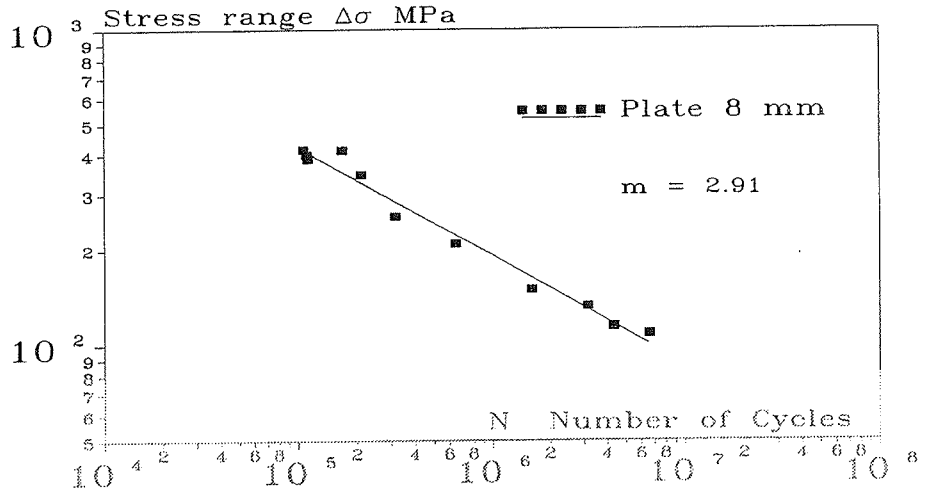

Figure 4.12 *Test results from specimens with t=8 mm*

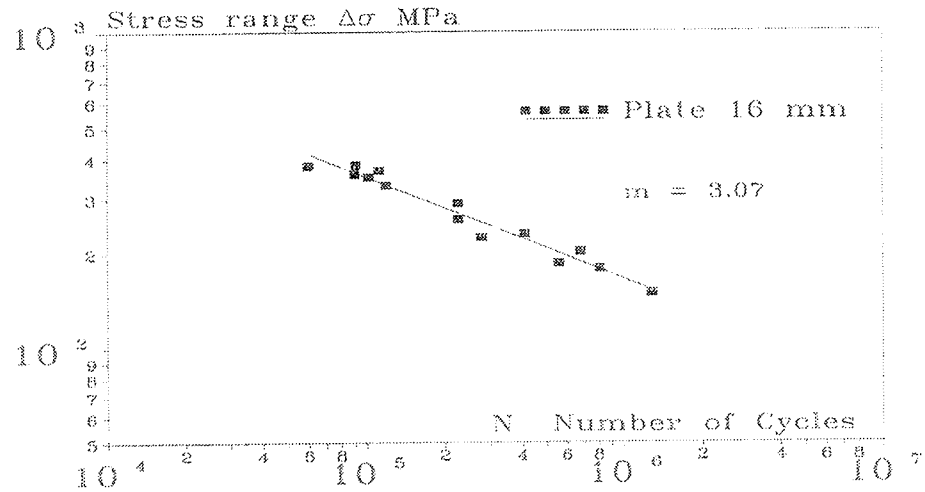

Figure 4.13 *Test results from specimens with t=16 mm*

Chapter 5

Comparison of test results with theory

5.1 Introduction

In this chapter the tests results presented in chapter 4 will be compared with the results from the crack propagation formula. A comparison with two kinds of welded connections will be carried out.
Firstly a comparison with a test series of Welded Center Cracked Test specimen (WCCT) will be treated using the da/dN-ΔK_i curve approach. The specimens in this test series are welded in different directions compared to the crack growth direction. The purpose is to observe the effect of residual stresses upon the crack growth rate, and to examine whether the crack propagation formula can predict this effect.
Secondly a comparison with Fillet Welded Joint Test specimens is carried out. This type of welded connection is very often used in structures. It is the aim to investigate how exact the crack propagation formula can predict the service life of the fillet welded joint by using the S-N-diagram approach. The method used will be to predict the number of cycles at failure N_f for different stress levels.

5.2 Welded Center Cracked Test specimen (WCCT)

In this section the test results from the Welded Center Cracked Test specimens will be compared with results from the crack propagation formula. Firstly a reference calculation will be performed. This will be compared with the test specimen U, which is not welded. Secondly the residual stresses will be taken into account in the formula to predict the crack propagation in the Welded Center Crack Test

specimens P and L. The specimen L is welded perpendicular to the crack growth direction, and it is therefore expected that the residual stresses only will have influence in the early state of crack propagation. On the contrary the specimen P is welded longitudinally along the crack growth direction, and it is therefore expected that the residual stresses will have full influence in the whole fatigue life of the specimen.

As described in section 2.3, K_{IC} depends on the stress intensity factor K_I. Therefore it is necessary to determine the parameters M' and n'. In section 4.2 we observed that the test results had a slope corresponding to the Paris m value about 4.3, see figure 4.3. This is in the range of what is normally observed for medium strength steels.
From equation (2.30) we hereby get:

$$n' = 2 - \frac{1}{2} \cdot 4.3 = -0.15 \tag{5.1}$$

In section 4.2 K_{IC} was estimated to be $K_{IC}=120$ MN/m$^{3/2}$ which gives:

$$M' = \frac{120}{120^{-0.15}} = 246 \tag{5.2}$$

These values will be used in the following.

We also need the ultimate strength of the material. The ultimate strength is highly dependent on size effects due to the very small plastic zone in front of the crack tip which leads to higher strength in the plastic zone than that measured in laboratory tests. The phenomenon is described in detail in the earlier work by the author [94.1], and will only be summarized here.

The size effect is taken into account using Weibull's size effect law, **[39.1]** and **[39.2]**, together with information on the atomic strength of the material. Weibull's size effect law may be written:

$$f_u = c\,V^{-\frac{1}{n}} \tag{5.3}$$

where the empirical parameters c and n may be determined on the basis of the atomic strength and the usual laboratory strength by the following formulas, see **[94.1]**:

$$n = \frac{19.8}{\log\left(\frac{f_u^{\text{atomic}}}{f_u^{\text{laboratory}}}\right)} \tag{5.4}$$

$$c = f_u^{\text{laboratory}} L_0^{\frac{3}{n}}$$

Here f_u is the ultimate strength. The formula is used both for the yield strength f_y and the fracture strength f_t. The length L_0 is the length of a standard laboratory test specimen which is put to 10^{-2} m when determining the yield strength. The length is reduced with 30% to $L_0=7\cdot10^{-3}$m due to the necked area when determining the fracture strength f_t.
The atomic fracture strength for steel is, see **[94.1]**:

$$f_t^{\text{atomic}} = 32000\text{MPa} \tag{5.5}$$

The atomic yield strength may be put equal to:

$$f_y^{\text{atomic}} = 8300\text{MPa} \tag{5.6}$$

The laboratory yield strength and fracture strength have already been given in section 4.3.

The laboratory fracture strength $f_t^{laboratory}$ has to be increased with about 20% due to the fact that in a test we often get a combination of sliding failure along the edge and a separation failure in the necked area, and the cleavage strength therefore will be higher than the average stress measured over the necked area. Thus we have

$$f_t = 1.2\, f_{true\,fracture\,strength} \tag{5.7}$$

The laboratory yield strength $f_y^{laboratory}$ has to be increased by a factor 2.4 due to the fact that in plane strain the yield strength exceeds the uniaxial yield strength considerably. If the linear elastic stress distribution around a sharp crack is taken as the basis, the yield strength in plane strain is found to be 3 times the uniaxial yield strength **[86.1,p 115]**. Irwin suggested to use a factor of 1.68,**[60.2]**. In **[90.1]** the factor used was 2.4, a value which has been determined on the basis of finite element calculations. Since this is probably the best estimate, we will use it here, i.e.,

$$f_{y\,plane\,strain} = 2.4\, f_{y\,uniaxial} \tag{5.8}$$

This factor does not affect the determination of the Weibull parameter n, because n is determined on the basis of the actual uniaxial strength, but it does effect the determination of c which describes the actual stress condition in the actual case. According to formula (5.4) we get the following Weibull parameters for the fracture strength:

$$n = \frac{19.8}{\log\left(\frac{32000}{1.2\cdot 784}\right)} = \underline{12.6}$$

$$c = 1.2\cdot 784\cdot(7\cdot 10^{-3})^{\frac{3}{12.6}} = \underline{296} \tag{5.9}$$

and for the yield strength:

$$n = \frac{19.8}{\log\left(\frac{8300}{625}\right)} = \underline{17.6}$$
$$c = 2.4 \cdot 625 \cdot (10^{-2})^{\frac{3}{17.6}} = \underline{684} \qquad (5.10)$$

Instead of using the Weibull roots **n** referring to the volume scale it has been suggested in **[90.1]** to use the length scale roots **n/3**. When this is done the effective crack length term $a'_p = l_e$ might be used to determine the fracture strength f_t at the crack tip and the plastic zone length a_y may be used to calculate the yield stress at the crack tip, see also **[94.1]**.
From **[94.1]** we have the following equations for the calculation of the ultimate strengths:
The formula for the yield strength is:

$$f_y = \left[c \left(\frac{K_I^2}{2\pi} \right)^{-\frac{3}{n}} \right]^{\frac{1}{1-\frac{6}{n}}} \qquad (5.11)$$

For the tensile strength we have:

$$f_t = \left[c \left(\frac{K_I^2}{2\pi f_y} \right)^{-\frac{3}{n}} \right]^{\frac{1}{1-\frac{3}{n}}} \qquad (5.12)$$

Using this approach it is often found that the theoretical yield strength f_y exceeds the fracture strength f_t. In this case it may be assumed, that $f_y = f_t$ at the crack tip.
The ultimate strengths depend on K_I, because the size of the plastic and fracture zone length depend on K_I, see section 2.2. K_I may be chosen as an average value in the actual interval. In our case K_I varies from about 20 $MN/m^{3/2}$ to 50 $MN/m^{3/2}$. As an average we may put $K_I = 35$ $MN/m^{3/2}$ in the calculations.
Using formulas (5.11) and (5.12) we get the ultimate strengths:

$$f_y = 5120\ \text{MPa}$$
$$f_t = 4470\ \text{MPa} \qquad (5.13)$$

Since f_t is found less than f_y we must use:

$$f_y = f_t = 4470 \text{ MPa} \tag{5.14}$$

Two test series were carried out in **[79.1]** with different stress ratios $R=\sigma_{min}/\sigma_{max}$. The load conditions are listed in table 5.1:

	$R=\sigma_{min}/\sigma_{max}$	$\Delta\sigma$ MPa	σ_{min} MPa	σ_{max} MPa	P_{min} kN	P_{max} kN
Series 3	0.35	111	59	170	35	102
Series 4	0.5	107	107	214	64	128

Table 5.1 *Load conditions for the specimens in series 3 and 4 respectively, [79.1].*

In the following the parameters shown in table 5.2 will be used to predict the crack propagation behaviour of the WCCT specimens:

D	$2a_0$	M'	n'	f_y	f_t
3 mm	14 mm	246	-0.15	4470 MPa	4470 MPa

Table 5.2 *Parameters for Welded Center Cracked Tests.*

In table 5.2 a_0 is half the initial crack length, D the diameter of the hole at the crack center, see figure 4.1.
Consider first the reference specimen U, which was not welded. In section 2.3 the influence of the R-ratio was discussed and a new approach to take into account the R ratio effect was suggested.
In figure 5.1 the test results from series 3 and 4 are compared with Forman's equation and the new proposal.
The values C, n and K_{IC} used in Forman's equation (2.32) are 1.69E-9, 2.54 and 108MN/m$^{3/2}$ respectively. These values are based on a best fit taken from **[79.1]**.
The results found using the Energy Crack Propagation formula (ECP) are based on the parameters shown in table 5.2.

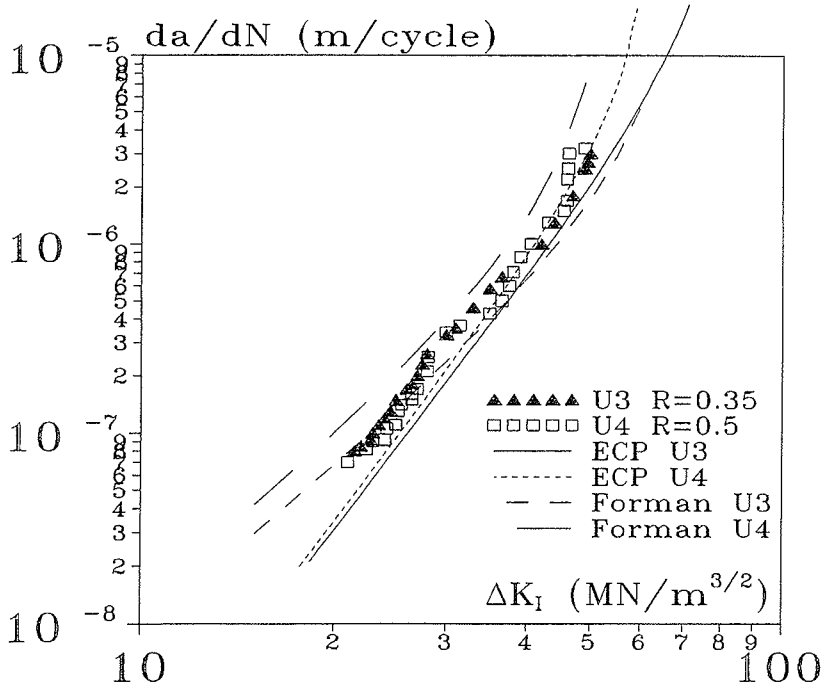

Figure 5.1 *Theory compared with test results, specimen U.*

It appears that Forman's formula gives too high crack growth rate for the specimen U4. The test results give almost identical crack growth rates, and it is observed that the new approach to take the R ratio into account gives very good results.
The results from ECP predict a little less crack growth rate than found in the experiment. This might be regulated with a slightly higher choice of the average value of K_I, when determining the ultimate strengths. Within normal expected uncertainty it must be concluded that ECP gives very accurate results. Contrary to Forman's formula, we also observe that close to failure ($K_{Imax} = \Delta K_I/(1-R) \approx K_{IC} = 120$ MN/m$^{3/2}$) ECP predicts that specimen U4 should fail before specimen U3 as observed, see figure 2.3.

In figure 5.2 a comparison between the test results for specimen P, welded perpendicular to the load direction, and the Energy Crack Propagation formula (ECP) is shown. In section 4.2 it was observed that the residual stress field, which is dominated by the tension stress field, increased the crack growth rate in the whole ΔK_I range. It appears that, by using the procedure described i section 3.2 and 3.3, the ECP-formula shows extremely good accordance with the test results. This means that the effect from different R ratios is taken into account so similar crack growth rates are obtained in the two test series. It may be concluded that the energy crack propagation formula is able to take the effects from the residual stresses into account.

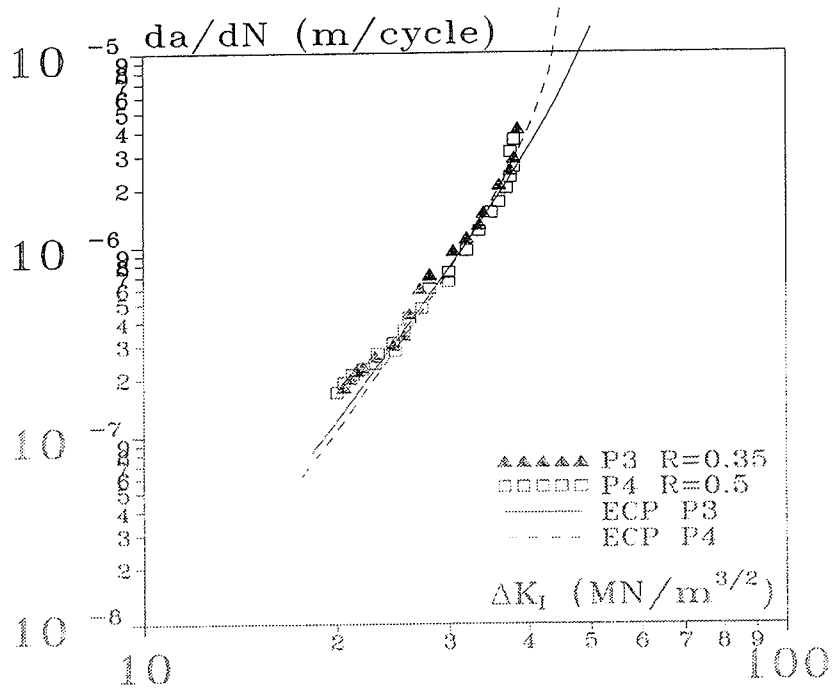

Figure 5.2 *Theory compared with test results, specimen P.*

In specimen P there are no effects from the residual compression field neither in the test results nor in the calculated results. This is due to the fact that the residual compression stresses only are active very close failure, where the crack growth rate is very high. This is contrary to the specimen L, welded longitudinally to the load direction. In the begining of crack propagation the residual tension stress field is active, but after some crack propagation the residual compression stress field is becoming active and reduces the crack growth rate. In figure 5.3 a calculation with ECP has been compared with the test results. We observe that the calculated crack

growth rate follows the same pattern as the tests results. For $\Delta K_I \approx 25$ MN/m$^{3/2}$ the crack growth rate starts to relaxe, both in theory and tests, due to the residual compression stresses.

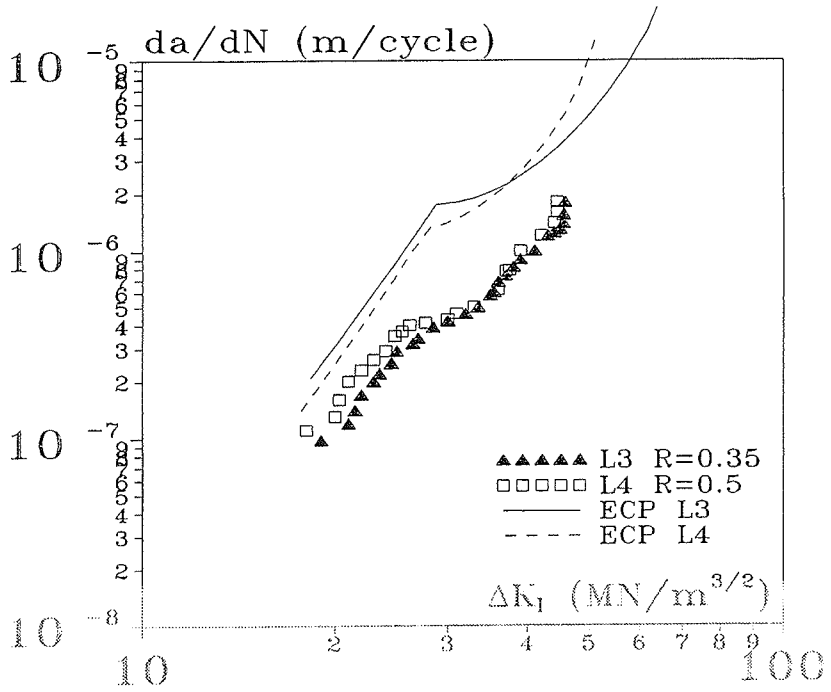

Figure 5.3 *Theory compared with test results, specimen L.*

However the theory predicts far too high crack growth rates. Forman's formula also to a certain degree gives too high predicted crack growth rates, especially for specimen L4, see **[79.1]**. This might be explained by the very high residual stress field in the center of the specimen. It is a fact that the tests results from specimen L follow the test results from specimen P in the low ΔK_I range. Therefore the effective residual stress field is lower than the values given in table 4.2.

It is known that if the residual stresses plus external load is close to the yield strength the effect from the residual stress field will be relaxed. However this is not a very likely explanation in this case, because the yield strength equals $f_y = 625$ MPa and $\sigma_r+\sigma_{smax} = 118 + 214 = 332$ MPa $< f_y$.

If the residual stress field is not relaxed by yielding or other reasons, then the most likely explanation is that the residual stresses measured have been overestimated, when using the approximation with a constant stress field.

If the residual stresses decrease very fast, as in the case of specimen L, it wil be more accurate to aproximate the residual stress field with a descending linear stress function. In appendix D a relation for a linear residual stress field has been derived, and it is shown that a constant stress of about 80 MPa in the tension region would be more accurate.
An estimate of the effective residual stress field on the basis of the approximate linear stress fit, and the fact that specimen L follows specimen P in the low ΔK_I range, is given in table 5.3:

	Specimen L	
crack interval	0-20 mm	20-75 mm
σ_r^{yy}	≈ 80 MPa	≈ -30 MPa

Table 5.3 *Estimated residual stress field, specimen L.*

Using this residual stress field we find the crack growth rates shown in figure 5.4.

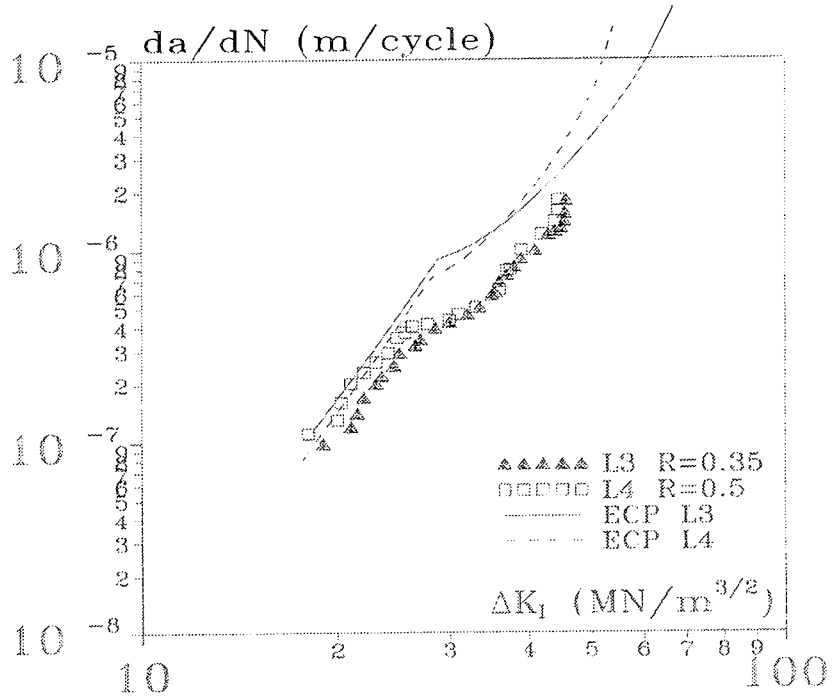

Figure 5.4 *Theory compared with test results, specimen L.*

Now the theory gives good accordance with the test results in the low range of ΔK_I, but still not for higher values of ΔK_I. The crack growth rates for specimen L3 seem to relaxe at $\Delta K_I \approx 25$ MN/m$^{3/2}$, while the theory predicts a relaxation at $\Delta K_I \approx 29$ MN/m$^{3/2}$. For a maximum load of $\sigma_{max} = 170$ MPa, we have $\Delta K_I = 29$ MN/m$^{3/2}$ and $K_{Imax} = 44$ MN/m$^{3/2}$. These values correspond to a crack length a $\approx$ 21 mm. This is in accordance with the crack interval given in table 5.3 showing that the residual tension stress field will start to be relaxed at a = 20 mm. However the test results indicate that this takes place for $\Delta K_I = 25$ MN/m$^{3/2}$ and $K_{Imax} = 38$ MN/m$^{3/2}$, which corresponds to a crack length of about 16 mm. Therefore it must be concluded that the residual compression field starts to be active for a crack length of about 16 mm in this specific test.

	Specimen L	
crack interval	0-16 mm	16-75 mm
σ_r^{yy}	$\approx$ 80 MPa	$\approx$ -30 MPa

Table 5.4 *Estimated residual stress field, specimen L.*

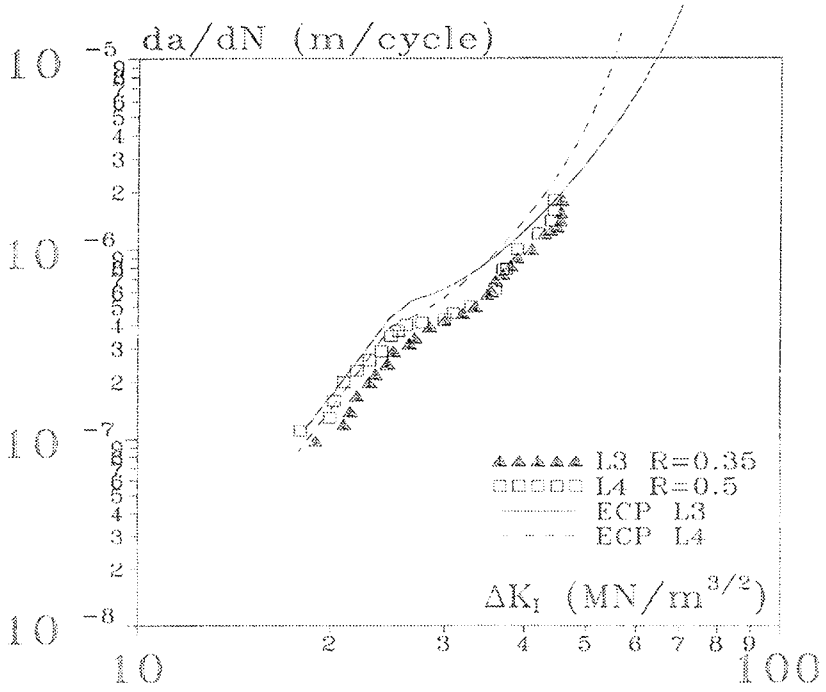

Figure 5.5 *Theory compared with test results, specimen L.*

In figure 5.5 a calculation with the residual stress field given in table 5.4 is presented. Comparing with figure 5.4 we observe that the result is very sensitive to the transition point between tension and compression. Further we observe that the transition point a_0 = 16 mm gives extremely good accordance between test and theory.

Finally a comparison between tests and theory for the whole test series 3 and 4 is shown in figures 5.6 and 5.7. The crack growth rates for specimen L3 and L4 are determined on the basis of the residual stress field given in table 5.4.

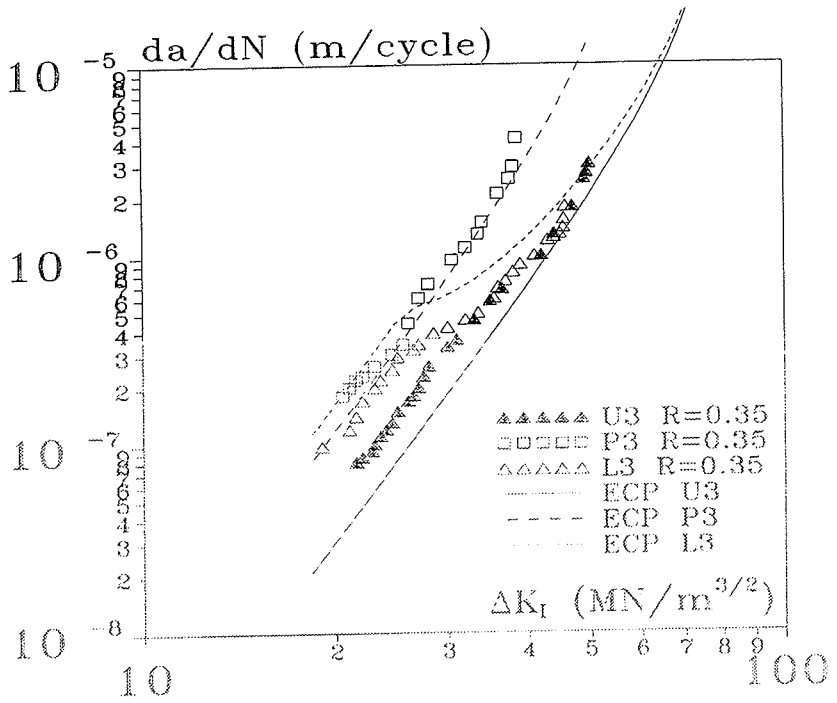

Figure 5.6 *Theory compared with test results. specimen L.*

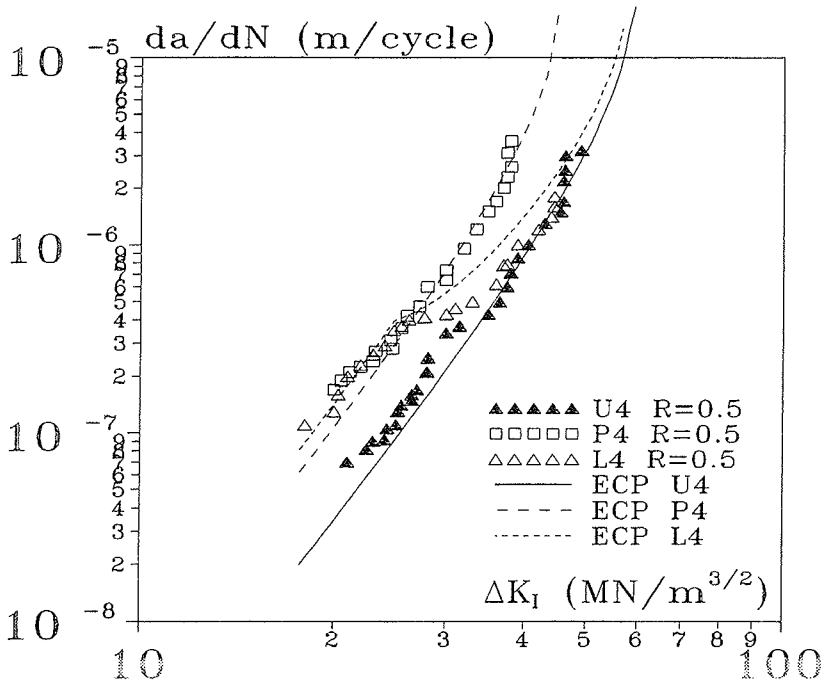

Figure 5.7 *Theory compared with test results, specimen L.*

It must be concluded that the Energy Crack Propagation formula (ECP) gives very good results when compared with test results.

5.3 Welded Joint Test specimen (WJT)

In this section the test results for the Welded Joint Test specimens will be compared with calculations. Firstly some basic parameter studies will be performed, and a definition of the standard parameters used will be established. Secondly the effect from the residual stress field will be taken into account.
In section 3.3 a formula to determine the stress intensity factor was presented, see equation 3.1. The stress gradient correction factor F_G is determined by equation (5.15), see also equation (3.3):

$$F_G = \frac{SCF}{1+\frac{1}{d}\left(\frac{a}{t}\right)^q} \qquad (5.15)$$

In this case the stress concentration factor SCF and the parameters d and q will be estimated on the basis of FEM calculations described in **[90.2]**, see appendix B. It has to be noted that the two weld toes have different geometry, see figure 4.8. The crack will propagate at the weld toe with the largest stress concentration, i.e. the crack will propagate at the weld toe 2 and the weld toe 4 in plate 16 and 8 mm respectively, see appendix B.
The stress concentration factor SCF equals F_G when the crack length a=0. From appendix B we therefore get SCF=2.543 for plate 16 mm. If we compare this with formula (3.4), having a weld toe width l=3 mm, we get SCF=2.785. We observe a close similarity. The small difference may be explained by the fact that the geometry of the weld toe is not symmetrical, see figure 4.8.
In the same way we find SCF=2.189 for plate 8 mm, see appendix B.
In **[85.1]** it is stated that F_G equals 1 for a/t>=0.325. This is in agreement with the FEM calculations in appendix B. Taking the middle crack point for instance at a/t=0.125 (corresponding to a=2 mm for plate 16 mm), the constants d and q can be determined using formula (5.15) and appendix B.
For plate 16 mm we have

$$1 = \frac{2.543}{1+\frac{1}{d}(0.325)^q} \quad \wedge \quad 1.141 = \frac{2.543}{1+\frac{1}{d}(0.125)^q}$$

$$\frac{1}{d} = \frac{1.543}{(0.325)^q} \quad \wedge \quad 1.141 = \frac{2.543}{1+1.543\left(\frac{0.125}{0.325}\right)^q} \qquad \textbf{(5.16)}$$

$$d = 0.4957 \quad \wedge \quad q = 0.2383$$

Similarly the following constants are found for plate 8 mm, taking the middle crack point in a=1.5 mm, and using SCF=2.189:

$$d = 0.6040 \quad \wedge \quad q = 0.2946 \qquad \textbf{(5.17)}$$

Hereby the stress gradient correction factor F_G can be calculated by formula (5.15) using the parameters shown in table 5.5:

	SCF	d	q
plate 16 mm	2.543	0.4957	0.2383
plate 8 mm	2.189	0.6040	0.2946

Table 5.5 *Parameters to determine the stress gradient correction factor F_G.*

The parameters recommended in **[85.1]** for non-load carrying fillet welded connections are very close to the values in table 5.5. The difference between the values is due to the fact that the geometry of the weld toe is not symmetrical, see figure 4.8. Furthermore a comparison with the method suggested and the FEM values shows very good agreement.

When solving the crack propagation formula to determine the number of cycles to failure N_f, the limits a_i and a_f in formula (3.16) have to be determined.
As described in section 3.3 the initial crack length a_i is put equal to $a_i = 0.2$ mm as an average value of measured notch values in welded connections.
The upper limit a_f can be estimated on the basis of K_{IC}. In section 4.3 K_{IC} was determined to be about $K_{IC} = 180$ MN/m$^{3/2}$. K_I depends upon the stress level. From the tests results, we have an average value of about $\Delta\sigma = 200$ MPa. Using formula

(3.1) we get the limits:

a_f = 7.9 mm for plate 8 mm

a_f = 15.5 mm for plate 16 mm

These limits give $K_I = K_{IC}$ for $\Delta\sigma$ = 200 MPa.

Both values are very close to the thickness of the specimen. In most tests failure will appear earlier due to static failure caused by yielding in the remaining area. Normally failure takes place for $a_f \approx 0.5 \cdot t$. This value will be used in the following. Furthermore it will be shown that if $a_f >> a_i$, then a small change in a_f does not affect the results very much.

As described in section 2.3 K_{IC} is a function of the stress intensity factor K_I. It is therefore necessary to determine the parameters M' and n'. In section 4.3 we observed that the test results showed a Paris m value of about m=3, see figures 4.12 and 4.13. This is in the range of what normally is observed for normal strength steel.

From equation (2.30) we hereby get:

$$n' = 2 - \frac{1}{2} \cdot 3 = 0.5 \qquad \textbf{(5.18)}$$

In section 4.3 K_{IC} was estimated to be K_{IC}=180 MN/m$^{3/2}$ which gives:

$$M' = \frac{180}{180^{0.5}} = 13.4 \qquad \textbf{(5.19)}$$

These values will be used in the following.

We also have to estimate the ultimate strengths of the material in the crack tip. This will be done using the same procedure as in section 5.2, i.e. the size effect is calculated using Weibull's size effect law, see formula (5.3). The empirical parameters c and n are determined on the basis of the atomic strength and the laboratory strength. By formula (5.4), we get the following Weibull parameters for the fracture strength:

$$n = \frac{19.8}{\log\left(\frac{32000}{1.2 \cdot 550}\right)} = \underline{11.7}$$

$$c = 1.2 \cdot 550 \cdot (7 \cdot 10^{-3})^{\frac{3}{11.7}} = \underline{185} \qquad \textbf{(5.20)}$$

and for the yield strength:

$$n = \frac{19.8}{\log\left(\frac{8300}{405}\right)} = \underline{15.1}$$
$$c = 2.4 \cdot 405 \cdot (10^{-2})^{\frac{3}{15.1}} = \underline{389} \qquad (5.21)$$

The ultimate strengths depend on K_I, because the size of the plastic and the fracture zone length depend on K_I, see section 2.2. K_I may be chosen as an average value in the interval in case. For instance in our case for plate 8 mm K_I varies from about 5 MN/m$^{3/2}$ to 23 MN/m$^{3/2}$, corresponding to a crack length varying from 0.2 mm to a_f = 4 mm. Contrary to earlier investigations with CCT specimens, **[94.1]**, K_I must be put equal to a value in the lower range of the interval, due to the very small initial crack length. In the case of welded joint connections most of the cycles to failure take place for very small crack lengths, i.e. the number of cycles to failure is highly dependent on the initial crack length. In table 5.6 it is shown that at least 4/5 of the total number of cycles to failure is used to extend the crack to half the crack length at failure (a = 2 mm) which corresponds to a K_I value of 14 MN/m$^{3/2}$. Therefore K_I must as an average be put equal to 8-10 MN/m$^{3/2}$. We use K_I = 9 MN/m$^{3/2}$. Then the ultimate strengths may be calculated by equation (5.11) and (5.12):

$$f_y = 8542 \text{ MPa}$$
$$f_t = 10515 \text{ MPa} \qquad (5.22)$$

a_i = 0.2 mm	Plate 8 mm	$\Delta\sigma$ = 200 MPa
a	K_I	N
1 mm	5	122400
2 mm	14	186500
4 mm	23	226300

Table 5.6 *Number of cycles as a function of the crack length. The number of cycles, N, has been determined using the parameters from table 5.7.*

In the following parameter study, the parameters used will be those determined in section 3.3 and above, see table 5.7:

a_i	a_f	M'	n'	a/b	f_y	f_t
0.2 mm	0.5·t	13.4	0.5	0.25	8542 MPa	10515 MPa

Table 5.7 *Parameters for Welded Joint Tests.*

Firstly it is important to verify that the numerical method used gives sufficient accuracy. Two numerical routines are used, one to solve the crack propagation formula and the other one to integrate numerically over the whole crack interval. The programme used is listed in appendix C. In table 5.8 calculated values of N_f (number of cycles to failure) are listed for different number of steps. It is observed that the Runge Kutta method used to solve the differential equation, the Crack Propagation Formula (ECP), is the most sensitive. It is concluded that a number of steps equal to 200 in both numerical calculations gives sufficient accuracy, having an error less than 2%.

Number of steps		$\Delta\sigma$=200 MPa
Solving the crack propagation formula	Numerical integration	N_f Cycles to failure
50	200	213000
100	200	221800
200	200	226300
400	200	228500
800	200	229500
200	100	226400
200	200	226300
200	400	226200

Table 5.8 *Examination of the influence of steps in the calculation.*

The influence of a change in the crack length at failure a_f is negligible as discussed earlier. In table 5.9 N_f has been determined for different values of a_f and it may be concluded that a choice of a_f equal to half the specimen width gives sufficient accuracy, having an error less than 5%. Notice that for $a_f >> a_i$ a change in a_f does not influence the result very much.

Plate 8 mm	$\Delta\sigma$=200 MPa		
a_f	4 mm	6 mm	7 mm
N_f	226300	235600	236700

Table 5.9 *Number of cycles to failure for different crack lengths at failure.*

On the contrary a change in the initial crack length a_i influences the result a lot. In table 5.10 the initial crack length is varied between 0.075 mm and 0.4 mm, which may be considered as a lower and an upper limit for the plate investigated, see section 3.3. The influence of the initial crack length is shown in figure 5.8.

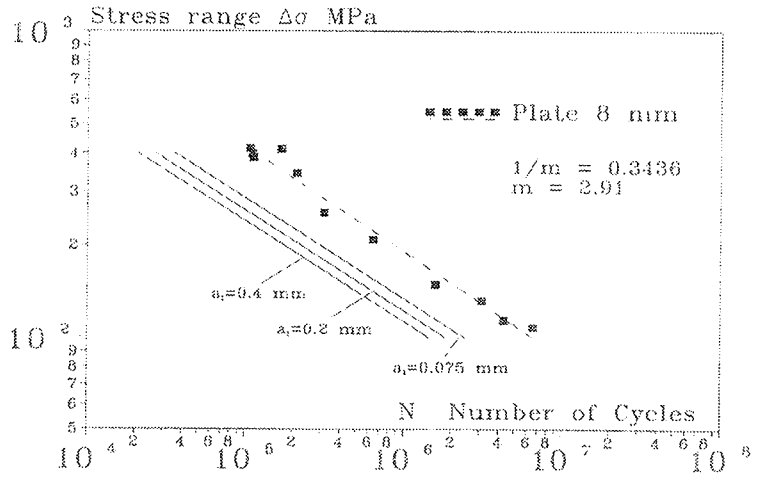

Figure 5.8 *Influence of initial crack length on fatigue life.*

Plate 8 mm $\Delta\sigma$=200 MPa				
a_i	0.075 mm	0.1 mm	0.2 mm	0.4 mm
N_f	299100	276600	226300	177000

Table 5.10 *Number of cycles to failure for different initial crack lengths.*

As may be seen in figure 5.9, the crack shape parameter a/b also has a large effect on the calculated fatigue lifes. The two extreme cases are a/b=1 which corresponds to a circular crack front and a/b=0.1 which corresponds to a linear crack front. In between we have elliptically shaped crack fronts.

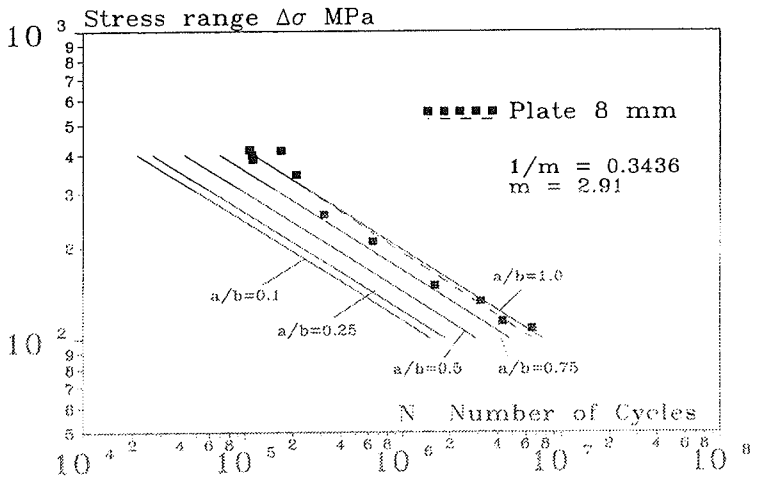

Figure 5.9 *Influence of the crack shape parameter a/b on fatigue life.*

Plate 8 mm $\Delta\sigma$=200 MPa					
a/b	0.1 mm	0.25 mm	0.5 mm	0.75 mm	1.0 mm
N_f	182900	226300	357700	583800	939400

Table 5.11 *Number of cycles to failure for different a/b ratios.*

Finally a comparison with the test results presented in section 4.3 will be produced. In the calculation we will take the residual stress field into account, using a similar method as in section 5.2. As seen from section 4.3, figures 4.10 and 4.11, the residual stress field in the tension zone can be aproximated by a linear stress field. Using the method described in appendix D, we find a residual stress field as given in table 5.12.

	Plate 8 mm			Plate 16 mm		
crack interval	0-2.4 mm	2.4-5.6 mm	5.6-8 mm	0-4.8 mm	4.8-11.2 mm	11.2-16 mm
σ_r^{yy}	60 MPa	-40 MPa	60 MPa	100 MPa	-55 MPa	100 MPa

Table 5.12 *Residual stress distribution in plate 8 mm and plate 16 mm respectively.*

Using the parameters in table 5.7 a calculation with the Energy Crack Propagation Formula is performed. In the figures 5.10 and 5.11 the test results for plate 8 mm and plate 16 mm are compared with a calculation including the residual stress field and a calculation neclecting the residual stresses.

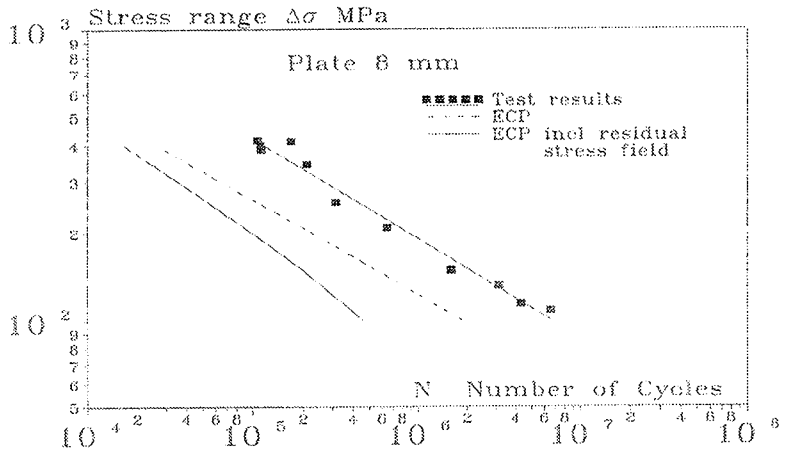

Figure 5.10 *Theory compared with test results, plate 8 mm.*

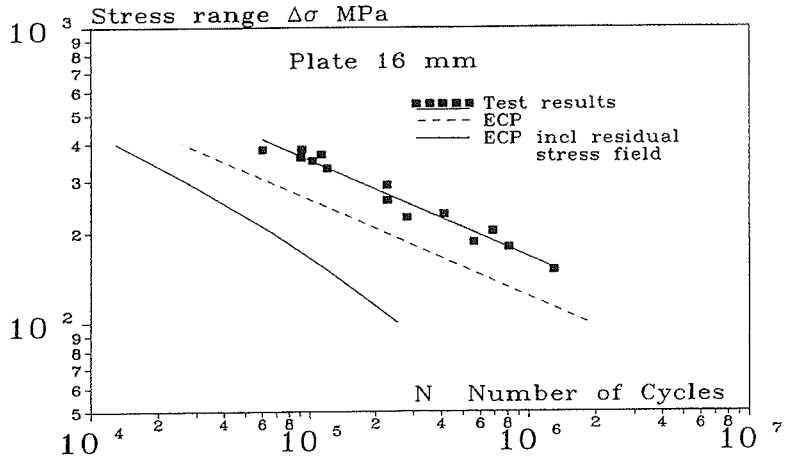

Figure 5.11 *Theory compared with test results, plate 16 mm.*

We observe in the figures 5.10 and 5.11 that the residual stress field reduces the fatigue service life of the specimen, as expected. The effect from the residual stress field is largest in the low stress range, where the residual stress field is more significant compared to the external load. It is further observed that the calculated fatigue life is smaller than the test results.
The reason cannot be an overestimation of the residual stress field, because it is observed that neclecting the effect of the residual stress field we still underestimate the fatigue life by the calculation.

The discrepancy might instead be explained by the crack closure phenomenon, described in section 2.3. If we take the effect from the crack closure into account, and determine the crack growth as a function of the effective stress intensity factor $\Delta K_{eff} = K_{Imax} - K_{op}$, where K_{op} is determined by equation (2.39) and (2.40) we get the fatigue life shown in figure 5.12 and 5.13.
Now we observe a very good accordance between test and theory. The calculated fatigue life is a little smaller than found in the tests. It may be explained by an overestimation of the residual stress field or it may be explained by the very rough model used to predict the effect from crack closure.

Further it is seen that ECP gives more accurate results in the low stress range. This may be explained by the fact that the residual stress effect is relaxed when the applied stress is close to the yield strength, as decribed in section 3.2.
The effect of crack closure has to be compared with more test results, before a final conclusion may be drawn. However, the results presented here show that taking this effect into account rather good results are obtained.

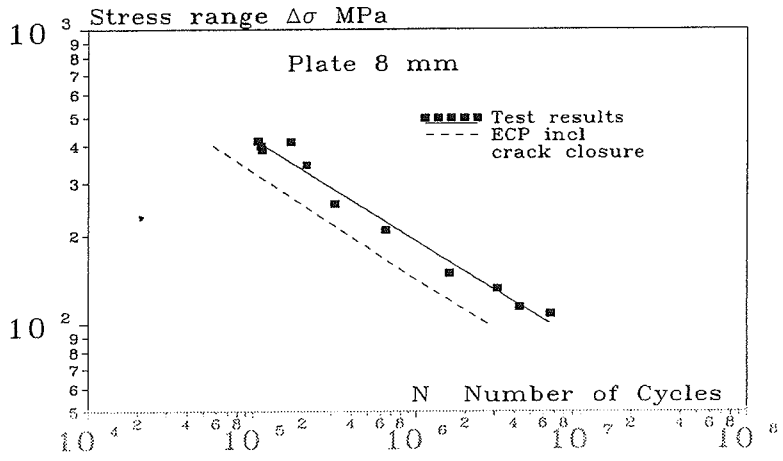

Figure 5.12 *Theory compared with test results, plate 8 mm.*

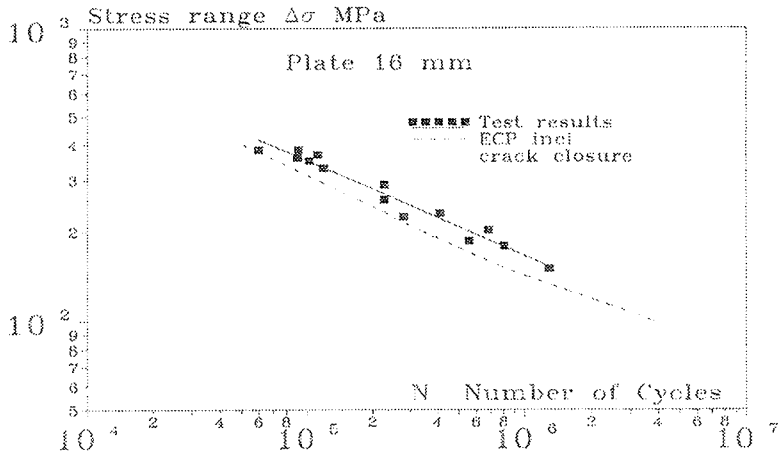

Figure 5.13 *Theory compared with test results, plate 16 mm*

Chapter 6

Conclusion

In the present investigation, the fatigue life of welded connections under constant amplitude loading has been studied. It has been the main purpose to examine the capability of the Energy Crack Propagation Formula (ECP) to predict crack propagation. Two tests series influenced by different parameters, such as residual stresses, the stress ratio R and crack closure are examined.

The overall conclusion is that ECP is able to predict crack propagation in welded connections and estimate the fatigue life very well.

A new method to take the influence of the R ratio into account has been derived. The method showed better results than those found by Forman's equation. Still a comparison with more tests has to be carried out before a final conclusion regarding the validity of the method can be made.

In the investigation of the WCCT specimen a large influence of the residual stress field was observed. In the paper an approximate method to take the residual stresses into account was introduced. Very good results were obtained both in the tension and in the compression residual stress field range. It was shown that ECP was able to predict the change of the crack propagation rate very precisely, when the minimum stress including the residual stress was less than zero. This might encourage to investigate the capability of ECP when applied to specimens with $R<0$ and, using a similar procedure.
The method is simple and may be used for practical applications, but more tests must be evaluated to ensure the general validity of the method.

It was shown that crack closure could be taken into account using a very simple empirical equation. Although the empirical relation is based on a large theoretical investigation the result can not be considered as a general way to describe the effect from crack closure. However, the method used does indicate that crack closure might be determined solely on the basis of the maximum stress level including the residual stress, and on the assumption that the minimum stress is less than the crack opening stress.

To fully understand the effect of residual stresses, R-ratio and crack closure, more research is still needed. It has been the purpose of this paper to present a new theory, to evaluate it, and hopefully to encourage the reader to apply it to other test conditions and thereby getting closer to the understanding of the behaviour of crack propagation in welded connections.

It may be concluded that the results obtained in this work look very promising.

Appendix A

Reference list

[21.1] A.A.Griffith,*The phenomena of rupture and flow in solids*, Phil.Trans.Soc.of London, A221, p 163-197, 1921.

[39.1] W.Weibull, *A statistical theory of the strength of materials*, Ingeniörvetenskapsakadamien. Handlingar nr 151, 1939

[39.2] W.Weibull, *The phenomenon of rupture in materials*, Ingeniörvetenskapsakadamien. Handlingar nr 153, 1939

[60.2] G.R.Irwin, *Plastic zone near a crack and fracture toughness*, Proc, 7th Sagamore Conf, p IV-63, 1960.

[63.1] P.C.Paris and F.Erdogan, *A critical analysis of crack propagation laws*, ASME, serie D, Vol 85, 1963.

[66.1] W.F.Brown and J.E.Srawley, *Plane Strain Crack Toughness Testing of High Strength Metallic Materials*, ASTM STP 410, p 1-66, 1966.

[67.1] R.G.Forman, V.E.Kearney, R.M.Engle, *Numerical analysis of crack propagation in a cyclic-loaded structure*, ASME Trans J. Basic Eng, p 459, 1967.

[70.1] W.F.Brown, *Review of developments in plane strain fracture toughness testing*, ASTM STP 463, 1970.

[71.1] H.F.Büeckner, *Weight functions for the notched bar*, Zeits. Angew. Math and Mech., vol 51, no 2, p 97-108, 1971.

[71.2] W.Elber, *The significance of fatigue crack closure,* Damage Tolerance in Aircraft Structures, ASTM STP 486, p 230-42, 1971.

[73.1] G.H.Sih, *Handbook of Stress Intensity Factors*, Bethlehem, Pennsylvania, Leheigh University, 1973.

[75.1] A.F.Grandt, *Stress Intensity Factors for Through Cracks at Fastener Holes*, Int.J.Fract, vol.11, p 283-294. 1975.

[76.1] D.P.Rooke and D.J.Cartwright, *Compendium of Stress Intensity Factors*, London, HMSO, 1976.

[77.1] S.T.Rolfe and J.M.Barsom, *Fracture and fatigue control in structures*, Application of Fracture Mechanics, Prentice-Hall Inc., 1977.

[77.2] P.Albrecht and K.Yamada, *Rapid Calculation of Stress Intensity Factors*, Journal of Structural Division, Proc. of the ASCE, Vol 103, No ST2, Feb 1977.

[79.1] G.Glinka, *Effect of Residual Stresses on Fatigue Crack Growth in Steel Weldments Under Constant and Variable Amplitude Loads*, ASTM STP 667, 1979, p 198-214.

[82.1] A.P.Parker, *Linear Elastic Fracture Mechanics and Fatigue Crack Growth - Residual Stress Effects*, in: Residual Stress and Stress relaxation (Editor E.Kula and V.Weiss), Plenum Publishers Corporation, New York, p 249-271, 1982.

[85.1] A.Almar-Næss, *Fatigue Handbook. Offshore Steel Structures*, Tapir, Trondheim, Norway, 1985

[86.1] D.Broek, *Elementary engineering fracture mechanics*, FractuREsearch Inc. Galena, OH, USA, 1986.

[89.1] K.Yamada and S.Nagatsu, *Evaluation of Scatter in Fatigue Life of Welded Details Using Fracture Mechanics*, Structural Eng./Earthquake Eng., Vol.6, No.1, pp 13-21, Japan Society of Civil Engineering (JSCE), April 1989.

[89.2] S.A.Meguid, *Engineering Fracture Mechanics*, Elsevier Applied Science, London, 1989.

[89.3] H.L.Pang, *Residual Stress measurements in cruciform welded joint using hole drilling and strain gauges*, Strain, Jour. of the British Soc. for Strain Meas., vol 25, no 1, Feb 1989.

[90.1] M.P.Nielsen, *An energy balance crack growth formula*, Bygningsstatiske Meddelelser, vol 61, nr 3-4, pp 71-125, Dansk Selskab for Bygningsstatik, Sept 1990.

[90.2] K.Yamada and H.Agerskov, *Fatigue Life Prediction of Welded Joints Using Fracture Mechanics*, Series R No 255, Department of Structural Engineering, Technical University of Denmark, 1990.

[91.1] H.H.Pedersen and T.C.Hansen, *Revneudvikling i stål*,(Crack propagation in steel), M.Sc.Thesis, Department of Structural Engineering, Technical University of Denmark, Feb 1991.

[92.1] J.B.Ibsø and H.Agerskov, *Fatigue Life of Offshore Steel Structures under Stochastic Loading*, Series R No 299, Department of Structural Engineering, Technical University of Denmark, Jan 1992.

[94.1] T.C.Hansen, *Fatigue and Crack Propagation, A new approach to predict crack propagation*, Series R 316, Department of Structural Engineering, Technical University of Denmark, May 1994.

[95.1] J.B.Ibsø, *Fatigue Life Prediction of Welded Joints Based on Fracture Mechanics and Crack Closure*, Series R No 322, Department of Structural Engineering, Technical University of Denmark, 1995.

[96.1] T.C.Hansen, *Fatigue in high strength steel, A new approach to predict crack propagation*, Series R 9, Department of Structural Engineering, Technical University of Denmark, November 1996.

[96.1] T.C.Hansen and D.H.Olsen, *Fracture and Crack Growth in concrete, A new approach to predict crack propagation*, Series R 11, Department of Structural Engineering, Technical University of Denmark, November 1996.

Appendix B

Geometrical correction factor F_G.

The number refers to weld toe 1, 2, 3 and 4 respectively, see figure 4.8.

a (mm)	Plate 16 mm 1	2	Plate 8 mm 3	4
0.0	2.407	2.543	2.123	2.189
0.1	2.233	2.345	1.973	2.026
0.2	1.957	2.021	1.733	1.756
0.4	1.642	1.662	1.460	1.455
0.7	1.434	1.442	1.281	1.275
1.1	1.295	1.297	1.162	1.157
1.5	1.213	1.210	1.092	1.088
2.0	1.151	1.141	1.039	1.035
3.0	1.083	1.068	1.000	1.000
4.0	1.043	1.028	1.0	1.0
5.0	1.013	1.003	1.0	1.0
6.5	1.000	1.000	1.0	1.0
8.0	1.0	1.0	1.0	1.0
10.0	1.0	1.0	-	-
12.0	1.0	1.0	-	-
16.0	1.0	1.0	-	-

Appendix C

Pascal programme solving the Crack Propagation Formula.

The programme takes residual stresses, crack closure and R-ratio into account.

The programme determines the fatigue life (number of cycles to failure). If the programme is used to determine the da/dN as a function of ΔK_I, neclect the procedure trapez and then run the programme for different choices of initial crack length ai.

Main procedures:

RUN:	Controles the main programme.
CRACKRATE:	Energy Crack Propagation Formula (ECP).
RUNGEKUTTA:	Solves the differential equation numerically.
TRAPEZ:	Numerical integration, determines the fatigue life.

```
programme ECP;

uses crt,dos,graph;

const
pi=3.141592654 ;

var
    clos                                    : real;
    leny                                    : real;
    q,d2,D,B,W,L,ra,s1,a,acr,ao,any         : real;
    astart,da,dda,sda,le                    : real;
    dadn                                    : real;
```

```
    ki1,ki2,kic1,dle,nk,mk,kstop                    : real;
    dp,rp,p,pmax,pmin,dadp                          : real;
    E,kmin,Kmax,ddk,dK,Kii,Gf,Kicbasis,fy,ft        : real;
    kitrans,kink,step1,step                         : real;
    ud,ud1,ind                                      : text;
    udfilnavn,udfilnavn1                            : string(.12.);
    j,i,valg,gammelfil,step2,stepsda,stop           : integer;
    m,y                                             : real;
    n,nn,nnn                                        : longint;
    delta,dd,FANE                                   : integer;
    ok,okud1,okud2,ok2,ok3,okstop,okud3             : boolean;
    tast                                            : char;
    k                                               : array[1..4] of real;
    c1,c2,c3,c4,modelk                              : real;
    indatafil,outputdatafil,outputdatafil1          : string(.12.);
    Fs,Fe,Fwt,Fg,elipse,sigma                       : Double;
    kr,a1,a2,a3,p1,p2,p3,sigma1,sigma2,sigma3       : double;
    Rs,Rres,sigmamax,sigmamin,sigmares              : double;
    ai,af,h                                         : double;
    f,fi,ff                                         : double;
    s,step                                      : integer;
    sum,intf                                        : double;

function pp(fa,fx :real ) :real;
 begin
 pp:=exp(fa*ln(fx));
 end;

function (*Stress intensity factor*)
   ki(fp,fa,fb,fw          : real)  :  real;
begin
 CASE fane of
  1:begin
  (* CCT*)
        y:=(sqrt(1/cos((pi*fa)/fw)));
        ki:=y*(sqrt(pi*fa)*fp/(fb*fw));
   end;
```

```
2:begin
(*CCT including hole around crack*)
        D:=0.004;
        y:=(0.94+(0.34/(0.14+(a-(D/2))/D)))*(sqrt(1/cos((pi*fa)/fw)));
        ki:=y*(sqrt(pi*fa)*fp/(fb*fw));
  end;

3:begin
(* Welded Joint *)

        Fs:=1.12-0.12*(elipse);
        Fe:=pp(-0.5,(1+4.5945*pp(1.65,elipse/2)));
        Fwt:=sqrt(1/(cos(pi*fa/(2*fw))));
         if ABS(fw-0.008)<1E-10 then begin
            d2:=0.3356;
            q:=0.5768;
            Fg:=2.189/(1+(1/d2)*pp(q,fa/fw));
            if Fg<=1 then Fg:=1;
           end;
           if ABS(fw-0.016)<1E-10 then begin
            d2:=0.2383;
            q:=0.4957;
            Fg:=2.543/(1+(1/d2)*pp(q,fa/fw));
            if Fg<=1 then Fg:=1;
           end;
        ki:=Fs*Fe*Fwt*Fg*sqrt(pi*fa)*fp/(fb*fw);
   end;
 end;
end;
function
   lp(fp,fa,fb,fw,ffy,fft     : real)   :   real;
 (* Plastic zone correction factor *)
 begin
   c1:=1/(2*pi);
   ki1:=ki(fp,fa,fb,fw);
   lp:=c1*sqr(ki1)/(ffy*fft);
 end;
```

```
function
    dlp(fp,fa,fb,fw,ffy,fft    : real)   :   real;
 begin
    c1:=1/(2*pi);
    ki1:=ki(fp,fa,fb,fw);
    c2:=1-(0.061*(fft/ffy));
    dlp:=c1*(2/fp)*sqr(ki1)/(ffy*fft);
 end;

function
    kic(fkmax                  : real)   :   real;
  (* Critical stress intensity factor *)
 begin
   if fkmax <= kitrans then
     begin
     kic:=kicbasis;
     end;
   if fkmax > kitrans then
     begin
     kink:=pp(nk,fkmax);
     kic:=mk*kink;
     end;
 end;

procedure outputdata;
(* write da/dN as function of ΔK_I *)
begin
  stepsda:=stepsda+1;
  if a > (acr-(sda*2)) then sda:=(acr-ao)/100;
  writeln(ud,ddk,dda,' ',nn,' ',le);
  writeln(ud1,kmax,kic1);
  a:=a+sda;
end;
```

```
procedure crackrate;

 begin
    (*Residual stresses*)
    p1:=sigma1*b*w;
    if ra+leny>a1 then begin
        p1:=(sigma1*b*w*(a1)+sigma2*b*w*(ra-a1))/ra;
      end;

    (* factor clos = crack closure *)
    clos:=1-0.3*(1+sigma1/sigma);

    le:=lp(clos*(rp+p1),ra,b,w,fy,ft);
    dle:=dlp(clos*(rp+p1),ra,b,w,fy,ft);
    ki1:=ki(clos*rp,ra,b,w);
    ki2:=ki(clos*rp,ra+le,b,w);
    kic1:=kic(clos*kmax);
    (*Residual stresses*)
    p1:=sigma1*b*w;
    kr:=ki(clos*p1,ra,b,w);
    if ra+leny>a1 then begin
        p2:=(sigma1*b*w*(a1)+sigma2*b*w*(ra-a1))/ra;
       kr:=ki(clos*p2,ra,b,w);
       end;
    ki1:=(ki1+kr);
    ki2:=(ki2+kr);
    kic1:=kic(kmax+kr);
(* Determination of crack increment by ECP *)
    dadp:=(sqr(ki1)*dle)
          /(sqr(kic1)-sqr(ki2));
 end;

procedure rungekutta;

 begin
   (* Determination of k-values *)
    k[1]:=1;
```

```
    j:=1;
   for i:=1 to 4 do
    begin
      m:=(trunc (i/2))/2;  (* values 0, 1/2, 1/2, 1 for i=1 til 4 *)
      rp:=p+m*dp;
      ra:=a+m*dp*k[j];
      Crackrate;
      k[i]:=dadp;
      j:=i;     (* To take into account the next a *)
    end;
   any:=a+(dp/6)*(k[1]+2*k[2]+2*k[3]+k[4]);
   {da:=any-a;}
   da:=(dp/6)*(k[1]+2*k[2]+2*k[3]+k[4]);
   if da < 0 then stop:=1;

end;

procedure run;

begin;
 a:=ao;
 kmax:=ki(pmax,a,b,w);
 kmin:=ki(pmin,a,b,w);
 ddk:=kmax-kmin;
 kii:=ddk;
 dp:=(pmax-pmin)/delta;

      writeln;
      writeln(' N= ',nn,' acr= ',acr:4:4,' a= ',a:4:4);}

    dd:=0;
    p:=pmin;
    dda:=0;
    kmax:=ki(pmax,a,b,w);
    kmin:=ki(pmin,a,b,w);
    ddk:=kmax-kmin;
    repeat        (* load is increased *)
```

```
        dd:=dd+1;
          p:=p+dp;
          rungekutta;
          leny:=le;
          dda:=dda+da;
          a:=a+dda;
    until (dd>=delta) or (p>=pmax) or (stop=1);
    dadn:=dda;
    outputdata; (* procedure write to file *)
end;

procedure trapez;

begin

  sum:=0;
  for s:=1 to (step-1) do begin
    write(s,' ');
    ao:=ai+s*h;
    run;
    f:=1/dadn;
    sum:=sum+f;
  end;
    ao:=ai;
    run;
    fi:=1/dadn;
    ao:=af;
    run;
    ff:=1/dadn;
   intf:=h*( 0.5*(fi+ff)+sum );
   writeln('Np = ',intf);
   writeln;

end;
```

```
procedure Zeroindata;
begin
fane:=0;
ok2:=false;okstop:=false;okud1:=false;okud2:=false;okud3:=false;
nn:=0;stepsda:=0;stop:=0;step2:=1;step:=1;
modelk:=0;b:=0;a:=0;w:=0;l:=0;pmin:=0;pmax:=0;e:=0;fy:=0;ft:=0;n:=0;
delta:=0;kicbasis:=0;kitrans:=0;nk:=0;mk:=0;
kr:=0;leny:=0;
a1:=0;a2:=0;a3:=0;p1:=0;p2:=0;p3:=0;sigma1:=0;sigma2:=0;sigma3:=0;
Rs:=0;Rres:=0;sigmamin:=0;sigmamax:=0;sigmares:=0;
indatafil:=' ';
outputdatafil:=' ';
outputdatafil1:=' ';
end;


Procedure indata;

begin

b:=0.090;   (* thickness *)
w:=0.016;   (* width *)
sigma:=100; (* maximum stress *)
pmin:=0;    (* minimum load *)
pmax:=sigma*w*b;
E:=210000;  {MPa=MN/m2}
fy:=9477;   {MN/m2}
ft:=fy;
delta:=200;  (* steps through one cycle *)
fane:=9;   (* 9 for welded joint stress intensity factor *)
kitrans:=0;   (* Limitation for Critical stress intensity factor *)

nk:=0.5;   (* Ki-kic parameters *)
mk:=13.4;  (* Ki-kic parameters *)

(*indata for trapez procedure*)
 elipse:=0.25;  {ratio between a og b,  elipse =a/b}
```

```
  step:=200;  (*total steps to failure*)
  ai:=0.0002; {m} (*initial crack length*)
  af:=0.008; {m} (*critical carck length*)
  h:=(af-ai)/step;  (*steplength*)

end;

procedure inresidual;
(*residual stresses*)
begin
  (*data for Glinkas WCCT test specimen u*)
{  a1:=0.075;
  a2:=0.075;
  sigma1:=0;
  sigma2:=0;}
  (*data for Glinkas WCCT test specimen P*)
{  a1:=0.044;
  a2:=0.075;
  sigma1:=62;
  sigma2:=-88;}
  (*data for Glinkas WCCT test specimen L*)
{  a1:=0.020;
  a2:=0.075;
  sigma1:=118;
  sigma2:=-43;}
  (*data for Glinkas WCCT test specimen L second calculation*)
{  a1:=0.016;
  a2:=0.075;
  sigma1:=80;
  sigma2:=-30;}
  (*data for Ibsøs WJT test plate 8 mm*)
{  a1:=0.0024;
  a2:=0.0056;
  a3:=0.008;
  sigma1:=80;
  sigma2:=-40;
  sigma3:=80;}
```

```
  (*data for Ibsøs WJT test plate 16 mm*)
{  a1:=0.0048;
  a2:=0.0112;
  a3:=0.016;
  sigma1:=130;
  sigma2:=-55;
  sigma3:=130;}

end;

{Mainprogram}

begin

zeroindata;
indata;
inresidual;
trapez;

  begin
    close(ud);
  end;

end.
```

Appendix D

Approximation of linear residual stress field.

In this appendix a formula to determine the residual stress intensity factor K_r on the basis of a linear residual stress field will be derived. An aproximation using a constant stress field will be proposed. The method may be used when the stress is varying very fast, since this reduces the effect from the residual stress as will be shown. The result is utilized for specimen L, which has a very steep stress field in the lower ΔK_I range, see section 5.2.
The stress intensity factor from a residual stress field σ_r^{yy} has been given in section 3.2, formula (3.10):

$$K_r = 2\sqrt{\frac{a}{\pi}}\int_0^a \frac{\sigma_r^{yy}(x)}{\sqrt{a^2-x^2}}dx \qquad \textbf{(D.1)}$$

If we assume a linear variation of the stress field, we have:

$$\sigma_r^{yy}(x) = \sigma_0 - \frac{\sigma_0}{a_0}x \qquad \textbf{(D.2)}$$

σ_0 being the residual stress at x = 0. Along the length a_0 the residual stress decreases to zero value. Substituting this into (F.1) we get

$$K_r = 2\sqrt{\frac{a}{\pi}}\left\{\sigma_0\int_0^a \frac{1}{\sqrt{a^2-x^2}}dx - \frac{\sigma_0}{a_0}\int_0^a \frac{x}{\sqrt{a^2-x^2}}dx\right\} \qquad \textbf{(D.3)}$$

The result is

$$K_r = \sigma_0\sqrt{\pi a} - \frac{2\sigma_0}{a_0\sqrt{\pi}}a\sqrt{a} \qquad \textbf{(D.4)}$$

If we insert the transition point between tension and compression, $a=a_0$, we get the simple result:

$$K_r = \sigma_0\sqrt{\pi a_0}\,(1-\frac{2}{\pi}) \qquad \textbf{(D.5)}$$

In the case of specimen L, the residual stress field was aproximated with a constant stress σ = 118 MPa, see figure 4.2. This corresponds to a stress intensity factor of $K_r = \sigma\sqrt{\pi a_0} = 29.6$ MN/m$^{3/2}$ at the transition point, (neclecting the geometrical correction factor β). If we instead assume a linear stress field having σ_0 = 200 MPa and a_0 = 20 mm we get from formula (F.5): K_r = 18.2 MN/m$^{3/2}$. This corresponds in a constant stress field to σ = 72.7 MPa, which is quite lower than the value used.
It is therefore suggested to reduce the residual stress field for the investigation of specimen L to a constant stress field with say σ = 80 MPa. This leads to an error only in the very low ΔK_I range. To obtain equilibrium it is suggested that the compression stresses are reduced to -30 MPa.

In the case of specimen P it is sufficiently accurate to approximate with a constant residual stress field without reduction, due to the shape of the residual stress field.

Dealing with the fillet Welded Joint Test specimens (WJT), see section 5.3, similarly a reduced constant residual stress field will be used. At the transition point a_0 = 2.4 mm for plate 8 mm, we have:

$$K_r = \sigma_0\sqrt{\pi a_0}\,(1-\frac{2}{\pi}) = 165\sqrt{\pi\,0.0024} = 5.2\,\text{MN/m}^{3/2} \qquad \textbf{(D.6)}$$

Using a constant residual stress field and demanding same stress intensity factor in the transition point we get the constant stress in the tension range:

$$\sigma = \frac{K_r}{\sqrt{\pi a_0}} = \frac{5.2}{\sqrt{\pi\,0.0024}} = 60\,\text{MPa} \qquad \textbf{(D.7)}$$

Similarly for plate 16 mm in the transition point a_0 = 4.8 mm:

$$\sigma = 275(1-\frac{2}{\pi}) = 100\text{MPa} \qquad \textbf{(D.8)}$$

To obtain equilibrium in the compression zone the stresses will be put equal to σ = -40 MPa for plate 8 mm and σ = -55 MPa for plate 16 mm.

Hvis De ikke allerede modtager Afdelingens resuméoversigt ved udgivelsen, kan Afdelingen tilbyde at tilsende næste års resuméoversigt, når den udgives, dersom De udfylder og returnerer nedenstående kupon:

Returneres til:

Institut for Bærende Konstruktioner og Materialer
Danmarks Tekniske Universitet
Bygning 118
2800 Lyngby

Fremtidig tilsendelse af resuméoversigter udbedes af
(bedes udfyldt med blokbogstaver):

Stilling og navn: . . . . . .

Adresse: . . . . . .

Postnr. og -distrikt: . . . . . .

*The Department has pleasure in offering to send you a next year's list of summaries, free of charge. If you do not already receive it upon publication, kindly complete and return the coupon below:

To be returned to:

Department of Structural Engineering and Materials
Technical University of Denmark
Building 118
DK-2800 Lyngby
Denmark

*The undersigned wishes to receive the Department's list of Summaries:
(Please complete in block letters):

Title and name: . . . . . .

Address: . . . . . .

Postal No. and district: . . . . . .

Country: . . . . . .